Universidade Nova de Lisboa

Instituto de Higiene e Medicina Tropical

Insights on the mechanisms underlying the development of heteroresistance to colistin in *Acinetobacter baumannii*

Sarah Gothe Esteves Viegas

A THESIS SUBMITTED IN PARTIAL FULFILMENT OF THE REQUIREMENTS FOR THE DEGREE OF MASTER IN MEDICAL MICROBIOLOGY

OCTOBER 2022

UNIVERSIDADE NOVA DE LISBOA

Universidade Nova de Lisboa
Instituto de Higiene e Medicina Tropical

Insights on the mechanisms underlying the development of heteroresistance to colistin in *Acinetobacter baumannii*

Author: Sarah Gothe Esteves Viegas

Supervisor: Doctor Diana Machado
Co-Supervisor: Professor Doctor Miguel Viveiros

Unidade de Ensino e Investigação de Microbiologia Médica; Instituto de Higiene e Medicina Tropical, Universidade Nova de Lisboa

A Thesis submitted in partial fulfilment of the requirements for the degree of Master in Medical Microbiology

Work partially funded by the Fundação para a Ciência e a Tecnologia (FCT), Portugal, through funding for the Global Health and Tropical Medicine Research Center (GHTM) Refª UID/Multi/04413/2013, project Ref. PTDC/BIA-MIC-30692/2017 (FCT), and program "Stimulus to Scientific Employment DL57" (FCT).

INSTITUTO DE HIGIENE E MEDICINA TROPICAL DESDE 1902

NOVA SCHOOL OF SCIENCE & TECHNOLOGY

NOVA MEDICAL SCHOOL

Acknowledgments

À orientadora deste projeto, Doutora Diana Machado, primeiramente pela oportunidade e voto de confiança em fazer parte deste projeto, pelo conhecimento partilhado nestes últimos três anos de trabalho que solidificaram a minha abordagem profissional para com o mundo científico e que se refletirá futuramente na minha carreira profissional. Obrigada pela disponibilidade em passar longas horas em dúvidas, revisões, pela orientação meticulosa e criteriosa para a elaboração deste trabalho e ainda pela amizade que coevoluiu nestes últimos anos, obrigada por tudo.

Ao co-orientador deste projeto, Professor Doutor Miguel Viveiros, por mais uma vez me dar a oportunidade e conceder um lugar neste projeto, pela sua boa disposição, e pelo voto de confiança nas minhas competências.

À Unidade de Microbiologia Médica do Instituto de Higiene e Medicina Tropical da Universidade Nova de Lisboa, agradeço a todos os colegas que tão bem me acolheram e partilharam este capítulo da minha vida.

À minha amiga Carolina Fernandes, que, desde que me lembro, sempre me apoiou com a sua amizade e conselhos sinceros, por compreender a minha ausência em muitos dos eventos de confraternização ocorridos neste período e pela força transmitida durante o mesmo.

À Isabel Roseiro pela sua amizade, boa disposição e camaradagem. Obrigada por partilhares comigo este período na minha vida. Que muitos mais momentos de cumplicidade e alegria nos aguarde. Entretanto percorremos caminhos diferentes com desafios diferentes, mas podendo sempre contar com o teu apoio.

A todos os amigos e colegas que acreditaram e valorizaram a realização deste trabalho, que não menciono aqui mas que não estão esquecidos.

Ao meu querido avô, que ficaria muito orgulhoso em compartilhar esse momento connosco.

A toda a minha família pelo apoio incondicional, conselhos, compreensão e força. Por partilharem esta experiência comigo e por sempre me desafiarem a tornar-me numa melhor versão de mim própria. Com vocês celebro esse momento tão especial e importante para mim.

Once again and this time in English for my family that does not understand Portuguese: To all my family for their unconditional support, sincere advice, understanding and strength. For sharing this experience with me and always challenging me to become a better version of myself. With you I celebrate this very special and important moment for me.

Ao meu irmão Thomas Viegas, que me deslumbrou durante este período com a sua personalidade desarmante, carinhosa e atenta. Obrigada por todo o apoio e força que muito me ajudou neste período.

Ao meu primo Jan Knoll, por estar presente todos os dias durante este período, por me apoiar com as suas palavras amigas e por me ajudar a olhar para os desafios sempre com uma perspetiva diferente.

Por fim, um agradecimento especial aos meus pais, a quem dedico este trabalho e sem os quais não teria tido a oportunidade de realizar este projeto. Pelo apoio incondicional, conselhos sinceros, compreensão, força e paciência. Por sentirem as minhas ansiedades assim como os momentos de felicidade o mais próximo à escala da realidade, por todo o apoio absoluto, obrigada.

Abstract

The versatility of intrinsic or acquired resistance mechanisms found in *Acinetobacter baumannii* is a constant challenge in combating infections caused by these bacteria. For the treatment of infections caused by multidrug-resistant (MDR) *A. baumannii*, colistin is usually the last therapeutic option. However, clinical isolates resistant to almost all available antibiotics, including colistin, have been reported worldwide. Some of these isolates also demonstrate the presence of heteroresistance to colistin, a phenomenon where there is a heterogeneous population with one or several sub-populations with different levels of antibiotic resistance compared to the main population in the same strain. The mechanisms underlying colistin heteroresistance are complex and diverse among different bacterial species, and poorly understood for *A. baumannii*. In this study, three isogenic strain-variants from a MDR *A. baumannii* carbapenemase-producing clinical isolate with simultaneous heteroresistance to colistin, strain-variant L, strain-variant S, and strain-variant XS, were characterized morphologically, phenotypic, and genotypically. Growth on colistin-supplemented Levine-agar revealed strain-variants exhibiting different colony morphologies that showed different colistin resistance profiles, different growth rates and stable heteroresistance phenotype. This data indicates that subpopulations heteroresistant to colistin could be selected upon antibiotic exposure. All variants showed increased efflux activity with different responses to the interactions between the efflux inhibitor thioridazine, colistin and ethidium bromide. The L variant and the S variant exhibited overexpression of the *adeG*, *craA*, *abeM* genes and the *abeS* gene in the S variant. Mutations in the *pmrB* gene, which encodes for the two-component PmrAB regulator involved in the lipopolysaccharide modification, and in the *lpxC* and *lpxD* genes responsible for lipid A biosynthesis were observed in all variants. This study evidenced the existence of more than one mechanism engaged in colistin heteroresistance in *A. baumannii*.

Keywords: *A. baumannii*; colistin; efflux; efflux pumps; heteroresistance.

Resumo

A versatilidade de mecanismos de resistência, intrínsecos ou adquiridos, encontrados em *Acinetobacter baumannii* são um constante desafio no que diz respeito ao combate às infecções provocadas por estas bactérias. Para o tratamento de infecções provocadas por estirpes de *A. baumannii* multirresistente (MDR), a colistina é geralmente a última opção terapêutica. No entanto, isolados clínicos resistentes a quase todos os antibióticos disponíveis, incluindo à colistina, têm vindo a ser reportados por todo o mundo. Alguns destes isolados apresentam ainda heterorresistência à colistina, um fenómeno que consiste na existência de uma população heterogénea com uma, ou várias subpopulações, com diferentes níveis de resistência ao antibiótico, em comparação com a população predominante da mesma estirpe. Os mecanismos subjacentes à heterorresistência à colistina são complexos e diversificados entre diferentes espécies bacterianas, e pouco compreendidos em *A. baumannii*. Neste estudo, três variantes isogénicas de uma estirpe de *A. baumannii* MDR, produtora de carbapenemases, com heterorresistência à colistina, variante L, variante S e variante XS, foram caracterizadas morfológica, fenotípica e genotipicamente. O crescimento em meio Levine-agar suplementado com colistina revelou diferentes morfologias de colónias entre as variantes, que por sua vez apresentam diferentes perfis de resistência à colistina, diferentes taxas de crescimento, e um fenótipo de heterorresistência estável. Estes resultados indicam que subpopulações heterorresistentes à colistina poderão ser selecionadas mediante exposição ao antibiótico. Todas as variantes apresentam um aumento da actividade de efluxo com respostas diferentes perante o inibidor de efluxo tioridazina, colistina e brometo de etídio. Nomeadamente, a variante L e a variante S demonstram sobreexpressão dos genes *adeG*, *craA*, *abeM* e também para o gene *abeS* na variante S. Mutações no gene *pmrB*, que codifica o regulador de dois componentes PmrAB envolvido na modificação de lipopolissacáridos, e nos genes *lpxC* e *lpxD* responsáveis pela biossíntese do lípido A foram observadas em todas as variantes. Este estudo evidência a presença de mais do que um mecanismo envolvido no desenvolvimento da heterorresistência à colistina em *A. baumannii*.

Palavras-chave: *A. baumannii*; colistina; efluxo; bombas de efluxo; heterorresistência.

Table of Contents

Acknowledgments i
Abstract iii
Resumo iv
Table of Contents v
Figure Index vii
Table Index viii
List of abbreviations ix
1. Introduction 1
1.1. The genus *Acinetobacter* 1
1.2. *Acinetobacter* pathogenicity 1
1.2.1. *Acinetobacter baumannii* clinical relevance 2
1.3. *Acinetobacter baumannii* treatment 3
1.4. Colistin effect *vs Acinetobacter baumannii* resistance mechanisms 5
1.5. Heteroresistance 6
1.5.1. Mechanisms underlying heteroresistance 7
1.5.2. Colistin heteroresistance 9
2. Material and Methods 10
2.1. Material 10
2.1.1. Biological material 10
2.1.2. Other biological material 10
2.1.3. Growth media and solutions 12
2.2. Methods 14
2.2.1. Growth and maintenance of bacterial strains 14
2.2.2. Morphological characterization 14
2.2.2.1. Morphological characterization by the Levine-agar method 14
2.2.3. Phenotypic characterization 15
2.2.3.1. Kirby-Bauer antibiotic susceptibility test (AST) 15
2.2.3.2. Colistin susceptibility testing by Etest 16
2.2.3.3. Determination of minimum inhibitory concentrations (MIC) by the 96-well microplate dilution method 17
2.2.3.3.1. MIC determination for colistin, efflux inhibitor and EtBr by the serial microdilution method in a 96-well microplate 17
2.2.3.3.2. Checkerboard assay to determination of COL and EtBr MIC in the presence of TZ, by the serial microdilution method in a 96-well microplate 18
2.2.3.3.3. MIC determination for colistin, thioridazine and EtBr by the macrodilution method in test tubes 19
2.2.3.4. Bacterial growth curve 19
2.2.3.5. Time-kill kinetic assay 20
2.2.3.6. Ethidium bromide accumulation assay 20
2.2.3.6.1. Cultures preparation 21
2.2.3.6.2. Accumulation assay 21
2.2.3.6.3. EtBr accumulation assay in the presence of efflux inhibitors 23
2.2.3.6.4. Ethidium bromide efflux assay 25
2.2.4. Genotypic characterization 26
2.2.4.1. Genomic DNA extraction 26

2.2.4.2. Enterobacterial repetitive intergenic consensus PCR (ERIC-PCR) fingerprinting 27
2.2.4.3. PCR amplification of efflux pump-encoding genes 28
2.2.4.4. PCR amplification and DNA sequencing of genes associated with colistin resistance 28
2.2.4.5. Efflux pump gene expression analysis 29
2.2.4.5.1. RNA extraction 29
2.2.4.5.2. RT-qPCR 30
3. Results and discussion 33
3.1. Morphological characterization of colonies by growth in SuperPolymyxin medium 33
3.2. Enterobacterial repetitive intergenic consensus PCR (ERIC-PCR) patterns 35
3.3. Colistin susceptibility testing by Etest 36
3.4. Growth curves of the *A. baumannii* strain variants 36
3.5. Resistance profile characterization and determination of minimum inhibitory concentration (MIC) 37
3.6. Chromosomal mutations screening in genes associated with colistin resistance. 40
3.7. Indirect detection of active efflux systems by checkerboard assays 41
3.8. Time kill assay for colistin 44
3.9. Detection of active efflux systems by the semi-automatic 96-well microplate fluorometric method 45
3.9.1. Detection of active efflux systems by the semi-automatic 96-well microplate fluorometric method 46
3.9.2. Evaluation of ethidium bromide accumulation in the presence of efflux inhibitor TZ 47
3.9.3. Detection of ethidium bromide efflux 49
3.10. Evaluation of expression levels of genes encoding for efflux pumps in response to colistin exposure by RT-qPCR 50
4. Final considerations 55
5. References 58
6. Appendix 68

Figure Index

Figure 1. Schematic representation of the preparation of strain suspensions and inoculation in SuperPolymyxin selective medium used for the morphological characterization of the strains under study…… **15**

Figure 2. Schematic representation of MIC determination by the serial microdilution method in a 96-well microplate……. **18**

Figure 3. Schematic representation of the 96-well plate preparation used for the ethidium bromide (EtBr) accumulation assays……. **22**

Figure 4. Schematic representation of the 96-well plate preparation used to perform the ethidium bromide (EtBr) accumulation efflux assay in the presence of the efflux inhibitor thioridazine (TZ)…… **24**

Figure 5. Schematic representation of 96-well plate preparation used in ethidium bromide (EtBr) efflux assay……. **25**

Figure 6. Morphological characterization of colonies by the Levine-agar method in SuperPolymyxin medium……. **34**

Figure 7. ERIC-PCR profile for each of the three strain variants and the parental strain Ab10-6 *A. baumannii* clinical isolate……..……. **35**

Figure 8. Image showing susceptibility test results obtained by Etest for the clinical strain Ab10-6 and its variants L, S and XS, plus ATCC19606 as a positive control……... **36**

Figure 9. Growth curves of the *A. baumannii* clinical strain Ab10-6, Ab10-6 variants L, S and XS, and reference strain ATCC19606, monitored for 24 h…… **37**

Figure 10. Death curves of the *A. baumannii* clinical strain Ab10-6, Ab10-6 variants L, S and XS, and reference strain ATCC19606, monitored for 24 h…… **45**

Figure 11. Determination of the equilibrium concentration of EtBr for the clinical strain Ab10-6, its variants and for the reference strain ATCC19606……. **46**

Figure 12. Effect of efflux inhibitor on EtBr accumulation in the absence of glucose……..…. **48**

Figure 13. EtBr efflux assay in the presence of the inhibitor of efflux systems……. **50**

Table Index

Table 1. Nucleotide sequences of primers used in molecular typing ERIC-PCR…. **10**

Table 2. Nucleotide sequences of primers used in efflux pump amplification……. **11**

Table 3. Nucleotide sequences of primers used in genes associated with colistin resistance amplification…… **11**

Table 4. Growth media composition…… **12**

Table 5. Composition and preparation of the solutions used…… **12**

Table 6. Composition and preparation of the buffer solutions used……. **12**

Table 7. Composition and preparation of substrate and efflux inhibitor solutions… **13**

Table 8. Composition and preparation of the antibiotic solution used……. **13**

Table 9. Antibiotics, concentrations, and breakpoints used in the Kirby-Bauer antibiotic susceptibility test……... **13**

Table 10. Preparation of SuperPolymyxin culture medium……. **14**

Table 11. Concentration range used in the determination of MIC through the serial microdilution method in a 96-well microplate…… **17**

Table 12. Colistin range concentration used in the determination of MIC through the serial macrodilution method…… **19**

Table 13. Colistin minimum inhibitory concentration (MIC) using different methods…… **39**

Table 14. Analysis of chromosomal mutations in genes associated with colistin resistance……. **40**

Table 15. EtBr and TZ minimum inhibitory concentration (MIC)…… **42**

Table 16. Colistin MIC values in the presence and absence of TZ and modulation factor (MF)……... **42**

Table 17. Ethidium bromide MIC values in the presence and absence of TZ and modulation factor (MF)…… **43**

Table 18. Relative final fluorescence (RFF) values obtained from the efflux inhibitor TZ and their standard deviation……. **48**

Table 19. Quantification by RT-qPCR of expression levels of genes encoding efflux pumps in *A. baumannii* strains and variants, in the presence of colistin at ¼ of the MIC……. **51**

List of abbreviations

Ab	*Acinetobacter baumannii*
AK	Amikacin
AMC	Amoxicillin/clavulanic acid
AMP	Ampicillin
ANF	Amphotericin B
AST	Antimicrobial susceptibility test
bp	Base pairs
C-	Negative control
C+	Positive control
CAZ	Ceftazidime
CC	Clonal complex
CDC	Center for Disease Control and Prevention
cDNA	Complementary DNA
CIP	Ciprofloxacin
CLSI	Clinical and Laboratory Standards Institute
CN	Gentamicin
COL	Colistin
Cq	Quantitation cycle
CRO	Ceftriaxone
CTAB	Cetyl trimethyl ammonium bromide
CTX	Cefotaxime
DAP	Daptomycin
DNA	Deoxyribonucleic acid
dNTP	Deoxynucleotide triphosphates
DO	Doxycycline
DOR	Doripenem
EDTA	Ethylenediamine tetraacetic acid
ERIC	Enterobacterial repetitive intergenic consensus
EtBr	Ethidium bromide
EUCAST	European Committee on Antimicrobial Susceptibility Testing
FEP	Cefepime
Fw	Forward
GC	Global clone
HCl	Hydrochloric acid
I	Susceptible, increased exposure
ICU	Intensive care units
IPM	Imipenem
LEV	Levofloxacin
LPS	Lipopolyssacharide
MDR	Multidrug resistant
MEM	Meropenem

MF	Modulation factor
MH	Minocycline
MHA	Mueller-Hinton agar
MHB	Mueller-Hinton broth
MIC	Minimum inhibitory concentration
mRNA	Messenger RNA
NADH	Nicotinamide adenine dinucleotide hydrogen
NET	Netilmicin
OD	Optical density
OX	Oxacillin
PBS	Phosphate buffered saline
PCR	Polymerase chain reaction
PDR	Pandrug or fully resistant
pH	Potential of hydrogen
PRL	Piperacillin
R	Resistant
RFF	Relative final fluorescence
RNA	Ribonucleic acid
RND	Resistance nodulation cell division
rpm	Revolutions per minute
rRNA	Ribosomal RNA
RT	Reverse transcription
Rv	Reverse
S	Susceptible
SNP	Single nucleotide polymorphisms
ST	Sequence type
SXT	Trimethoprim-sulfamethoxazole
TDR	Totally drug resistant
TE	Tetracycline
TGC	Tigecycline
TOB	Tobramycin
TZ	Thioridazine
TZP	Piperacillin-tazobactam
wt	Wild type
XDR	Extensively drug resistant

1. Introduction

1.1. The genus *Acinetobacter*

Acinetobacter genus belongs to the family *Moraxellaceae* consisting of 101 species (https://lpsn.dsmz.de/search?word=acinetobacter, accessed 12 September 2022). This genus has a long and convoluted taxonomic history. It was not until 1969 when Juni and Janik adopted the name *Acinetobacter* (coming from Greek akinetos [α + κίνητο + βακτηρ(ία)], meaning nonmotile rod) proposed by Brisou and Prévôt in 1954, that the classification *Acinetobacter* was confirmed and accepted by the "Subcommittee of the Taxonomy of Moraxella and allied bacteria". The genus *Acinetobacter* was formally accepted in Bergey's Manual of Systematic Bacteriology" in June 1984 (Bergogne-Bérézin, Friedman and Bendinelli, 2008).

Acinetobacter spp. are strictly aerobic Gram-negative coccobacilli, measuring 0.9-1.6 μm x 1.5-2.5 μm, becoming spherical throughout the stationary phase (Euzéby, 1997; Parte, 2018). Often found in coccoid pairs, these bacteria are nonmotile, non-spore formers, oxidase-positive and -negative, catalase producers, and not fermenting organisms. Bacteria included in this genus are ubiquitous organisms that could be find in different environmental settings like soil, water, food, sewage, and very importantly in clinical environment (Bergogne-Bérézin, Friedman and Bendinelli, 2008; Wong *et al.*, 2017).

Being nutritionally undemanding, with rare exceptions, gives them a greater growth capacity in most of the media used in laboratory routine. Most strains grow between 20ºC and 37ºC, although some are unable to grow at 37ºC. Therefore, the optimal growth temperature lies between 33°C and 35°C. Colonies are generally unpigmented and mucoid when the cells are encapsulated. Because they are usually found in pairs, they can form chains of variable size. They have a G+C DNA content between 38% and 47% (Euzéby, 1997; Parte, 2018).

1.2. *Acinetobacter* pathogenicity

The common species to cause infections in the diverse *Acinetobacter* genus is *A. baumannii*, which is described as the most virulent of all the species in this genus. Other pathogenic species of this genus are *A. lwoffii*, *A. calcoaceticus*, *A. haemolyticus*, *A.*

johnsonii, *A. junii*, *A. nosocomialis*, *A. pittii*, *A. schindleri*, and *A. ursingii* (Dijkshoorn and van der Toorn, 1992; Chusri *et al.*, 2014; Wong *et al.*, 2017). Moreover, there is another species consider as emerging pathogen in Asia called *A. seifertii* that is genetically close related to *A. baumannii* and may therefore be misidentified as such (Wong *et al.*, 2017).

But this genus harbours 101 different species, being most of them non-pathogenic environmental organisms with no clinical relevance. On the other hand, these environmental species can nonetheless act as reservoirs for antibiotic resistance genes, like extended-spectrum β-lactamases and carbapenemases, that can be transferred into clinically relevant species such as *A. calcoaceticus*, *A. lwoffii*, *A. nosocomialis*, and *A. pittii*, that have been detected on vegetables, meat, dairy products, and human skin (Bergogne-Bérézin, Friedman and Bendinelli, 2008; Wong *et al.*, 2017). As a result, extensive antibiotic resistance repertoires harbour in such strains, promoting various environmental transmission routes into human populations. Even *A. baumannii* strains harbouring extensive antibiotic resistance have been found to contaminate commercial food, including vegetables, meat, and multiple livestock types (Wong *et al.*, 2017).

The estimated occurrence of *Acinetobacter* infections globally per year is of 1 million (range, 600 000 to 1.400 000) (Spellberg and Rex, 2013). The infections can be acquired in the community and most frequently in hospital environments, considered as nosocomial infections. Nosocomial infections caused by *Acinetobacter* may occur either occasionally in the form of sporadic cases or as outbreaks (Bergogne-Bérézin, Friedman and Bendinelli, 2008).

1.2.1. *Acinetobacter baumannii* clinical relevance

A. baumannii is the species of the *Acinetobacter* genus with the most clinical relevance both for nosocomial and community-acquired infections, mainly due to its diverse antibiotic resistance mechanisms (Vrancianu *et al.*, 2020). *A. baumannii* can be a community-acquired infection with uncommon but important cause of community-acquired pneumonia. Most reported cases are associated with risk factors such as alcoholism, smoking, chronic obstructive pulmonary disease, and diabetes mellitus. Though, it has been observed almost exclusively in tropical climates, particularly in

Southeast Asia and tropical Australia (Falagas *et al.*, 2007; Peng, Zong and Fan, 2012), community-acquired *A. baumannii* lung infections, despite being less frequent than in hospital settings, tend to be more severe, leading to a mortality rate of 60% (Antunes, Visca and Towner, 2014). The high mortality associated with *A. baumannii* infections in the community is due to the difficulty in providing on time diagnosis and inadequate therapy. Although these *A. baumannii* strains circulating in the community are generally susceptible to most antibiotics used in therapy (Dijkshoorn, Nemec and Seifert, 2007; Falagas *et al.*, 2007). Furthermore, a characteristic manifestation of *A. baumannii* is wound infection associated with natural or man-made disasters such as earthquakes, bombing, and military operations, resulting in *A. baumannii* exposure and infection on deep-wound, burn-wound and osteomyelitis cases (Davis *et al.*, 2005).

Even though *A. baumannii* can be a community-acquired pathogen or responsible for infection associated with natural disasters and war casualties, nosocomial infections are the main cause of concern for this species. Being resistant to desiccation gives *A. baumannii* the ability to survive in hostile environments and persistence in healthcare settings, resulting in hospital-acquired *A. baumannii* infections such as ventilator-associated pneumonia, skin and soft-tissue infections, wound infections, urinary-tract infections, secondary meningitis, and bloodstream infections. These infections mainly occur in immunocompromised patients, patients who suffer from burns, have trauma and the highest density of infections occurs in intensive care units (ICUs) where patients stay for a longer period (Wong *et al.*, 2017). The mortality rate associated with *A. baumannii* infection in hospital settings is approximately 30% (Perez *et al.*, 2007). Due to the high morbidity and mortality associated with these infections and their high ability to acquire resistance to carbapenems, used as first-line therapy, these infections represent a major source of public health concern (World Health Organization, 2017).

1.3. *Acinetobacter baumannii* treatment

When confronting a pan-susceptible *A. baumannii* isolate, there may be several therapeutic options, including a broad-spectrum cephalosporin (like cefepime, ceftazidime, ceftriaxone, or cefotaxime), fluoroquinolones, (levofloxacin and ciprofloxacin), aminoglycosides (amikacin and tobramycin), an antibiotic in combination with a β-lactamase inhibitor (ampicillin/sulbactam), or carbapenems (imipenem and

meropenem) (Asif, Alvi and Rehman, 2018). However, *A. baumannii* has been endowed with the genetic setup for rapid development of antimicrobial resistance being intrinsically resistant to several antibiotics commonly used to treat Gram-negative bacterial infections (Asif, Alvi and Rehman, 2018). Consequently *A. baumannii* is one of the most resistant organisms found in clinical medicine, raising a challenge when it comes to provide an effective empirical therapy, resulting most often in treatment failure (Wong *et al.*, 2017). Thus, *A. baumannii* infections should be treated according to their resistance category, which are described as follows:

a) Multidrug resistant (MDR), when an isolate presents resistance to three or more classes of antimicrobials, such as β-lactams, fluoroquinolones, and aminoglycosides. Treatment of *A. baumannii* MDR infections is based on therapy with carbapenems, namely imipenem, meropenem or doripenem, as first-line treatment (Peleg, Seifert and Paterson, 2008; Manchanda, Sinha and Singh, 2010);

b) Extensively drug resistant (XDR), when presenting a MDR phenotype plus resistant to carbapenems. In such cases, second-line therapy is implemented with colistin (polymyxin E), tigecycline, minocycline or colistin in combination with doxycycline, rifampicin, or sulbactam (β-lactamase inhibitor). In the absence of colistin, a different therapeutic approach may be considered, such as administration of minocycline and meropenem in combination (Petrosillo, Ioannidou and Falagas, 2008; Vila and Pachón, 2008; Fishbain and Peleg, 2010; Manchanda, Sinha and Singh, 2010; Liang *et al.*, 2011; Viehman, Nguyen and Doi, 2014).

(iii) Pandrug or fully resistant (PDR), is an XDR isolate plus resistant to polymyxins and tigecycline (Kyriakidis *et al.*, 2021). Here deciding on a treatment regimen can be difficult due to lack of clear guidelines regarding the management of XDR *A. baumannii* infections (Kalil *et al.*, 2016). However, there are some options that show promising clinical improvements and clinical cure through the use of sulbactam combined with another single antibacterial agent (such as levofloxacin or tigecycline) (Liu *et al.*, 2021). Additionally, combinations of cefiderocol (a novel siderophore cephalosporin) plus sulbactam-durlobactam (β-lactam and β-lactamase inhibitor) have been shown to be a successful treatment of pneumonia and septic shock caused by XDR *A. baumannii* (Zaidan, Hornak and Reynoso, 2021; Durand-Réville *et al.*, 2017; McLeod *et al.*, 2020).

Yet, colistin-based combination therapy remains the most widely implemented therapeutic option to counteract these infections (Liu *et al.*, 2021).

1.4. Colistin effect *vs Acinetobacter baumannii* resistance mechanisms

MDR and XDR *A. baumannii* are responsible for most severe healthcare-associated infections worldwide being the main agent of ventilator-associated pneumonia corresponding to nearly 15% of all hospital-acquired infections, incurring the highest morbidity and mortality in medical wards and especially in the ICU. Plus their prevention and treatment are associated with high healthcare costs, counting for ~50% of the total use of antibiotics in the ICUs (Demirdal, Sari and Nemli, 2016; Asif, Alvi and Rehman, 2018; Liu *et al.*, 2021). The severity of *A. baumannii* infections results from the multiplicity of resistance mechanisms based on chromosomal mutations and the acquisition of antibiotic resistance genes through horizontal gene transfer, triggering drug inactivation/alteration through enzymatic modifications resulting in antibiotic neutralization, modification of drug target site, regulation of antibiotic transportation across bacterial membranes by modifying cell permeability, and biofilm formation (Vrancianu *et al.*, 2020; Kyriakidis *et al.*, 2021).

The target of polymyxins is the outer membrane of Gram-negative bacteria. *A. baumannii* being a Gram-negative bacterium, carries a semipermeable outer membrane, a bilayer structure with an inner leaflet resembling the cell membrane in composition, and an outer leaflet containing a distinctive component, a lipopolysaccharide (LPS) which is required for the function of many outer membrane proteins and serves to protect the cell. The LPS consists of a complex glycolipid, called lipid A, to which is attached a polysaccharide made up of a core and a terminal series of repeat units (Brooks *et al.*, 2012). This lipid A is negatively charged, allowing it to interact with the cationic lipopeptides of polymyxins B and E (widely known as colistin). This interaction results in destabilization of the outer membrane, uptake of the polymyxins into the periplasm, and increased permeability by disrupting the integrity of both outer and inner membranes leading to leakage of the cytoplasmic content and ultimately causing cell death, suggesting a detergent-like mode of action (Poirel, Jayol and Nordmann, 2017; Kyriakidis *et al.*, 2021). Another antibacterial mechanism is the neutralization of the LPS endotoxicity effect created during cell lysis through the binding ability of polymyxins to lipid A (Li *et al.*, 2005).

Furthermore, polymyxins can provide the inhibition of vital respiratory enzymes such as type II NADH-quinone oxidoreductases present in the bacterial inner membrane (Deris *et al.*, 2014; Poirel, Jayol and Nordmann, 2017).

A. baumannii resistance mechanisms to polymyxins include (i) drug target alteration through lipid A modification via mutations in the *pmrCAB* operon and *mcr* genes; (ii) mutations in *lpxA*, *lpxC*, and *lpxD* genes – responsible for encoding acyltransferases, essential to lipid A biosynthesis, and associated with lipid A deficiency; (iii) permeability defects, and osmotic resistance of the outer membrane associated with *lpsB*, *lptD*, and *vacJ* expression; (iv) lacking concentration of cofactors constitutional for LPS formation, like biotin, which are essential for susceptibility to polymyxins; and (v) efflux pump activity (Machado *et al.*, 2018; Kyriakidis *et al.*, 2021).

The increased use of colistin against MDR/XDR *A. baumannii* isolates worldwide has resulted in emerging colistin resistance (Chen *et al.*, 2020). Although the incidence of colistin-resistant strains remains low, it is increasing (Valencia *et al.*, 2009; López-Rojas *et al.*, 2011; Rolain *et al.*, 2011; Kim *et al.*, 2014; Machado *et al.*, 2018), which indicates that *A. baumannii* can cause infections that are fully refractory to the currently available antimicrobial armoury (Dijkshoorn, Nemec and Seifert, 2007). Colistin heteroresistance, a phenomenon corresponding to the emergence of a colistin-resistant subpopulation (that can grow in the presence of 4 g/mL of colistin) within a susceptible population (i.e., with a MIC $\leq$ 2 g/mL), has been observed for *A. baumannii* (Poirel, Jayol and Nordmann, 2017). This heteroresistance phenomenon raises concerns about subpopulations not being adequately targeted by colistin in an apparently colistin susceptible isolate. The emergence of resistance during therapy with colistin has been related with selection of heteroresistant subpopulations (Viehman, Nguyen and Doi, 2014).

1.5. Heteroresistance

The definition of bacterial heteroresistance broadly refers to the phenomenon in which a variability of response to antibiotics can be found among a bacterial population (El-Halfawy and Valvano, 2015). Here the presence of a heterogeneous population with one or several subpopulations can exhibit increased levels of antibiotic resistance when compared to the main population in the same culture (El-Halfawy and Valvano, 2015;

Andersson, Nicoloff and Hjort, 2019). Since its first designation in 1947 (Alexander and Leidy, 1947), many bacterial species have been described has displaying heteroresistance to different classes of antibiotics, whereby the resistant cells of the heteroresistant population can proliferate in the presence of the given antibiotic, and potentially result in treatment failure (Pereira *et al.*, 2021). To date, several reports have emerged describing the prevalence of heteroresistance among various bacterial species to various classes of antibiotics, and some experts maintain that heteroresistance is an underestimated phenomenon in both diagnosis and treatment of infectious diseases (El-Halfawy and Valvano, 2015; Andersson, Nicoloff and Hjort, 2019; Nicoloff *et al.*, 2019; Manjunath *et al.*, 2021; Pereira *et al.*, 2021).

Adding to this definition of heteroresistance provided by El-Halfawy and Valvano (El-Halfawy and Valvano, 2015), which focused on the presence of a subpopulation of resistant cells with an MIC at least eightfold higher than the highest concentration of the drug that does not affect growth of the main susceptible population, Andersson, Nicoloff and Hjort (Andersson, Nicoloff and Hjort, 2019) suggest several supplementary factors to be consider when studying and defining heteroresistance. Such factors include the origin, clonality, resistance level, resistance stability, and frequencies of the resistant subpopulations, as well as limitation of the heteroresistance phenotype to cases where the main population is clinically susceptible, to take into consideration the associated clinical complications regarding the treatment of these infections, since a resistant phenotype would be obtained by subjecting an isolate or a sample with a resistant main population to an antimicrobial susceptibility test (Andersson, Nicoloff and Hjort, 2019). However, this last premise may conflict with research studies on the mechanisms underlying heteroresistance in organisms that display a heteroresistant phenotype even with a main population considered as resistant, such as the present study.

1.5.1. Mechanisms underlying heteroresistance

The origin and clonality of resistant subpopulations are considered in the definition of heteroresistance, as resistant subpopulations may have different mechanisms resulting from different origins. For example, when in the presence of a co-infection where different clones consisting of a mixture of genetically distinct populations, exhibiting different levels of resistance, heterogeneity can occur. Similarly, if a rare spontaneous

resistant mutant increases in proportion in the population during an antimicrobial treatment, the heteroresistance phenotype could not be detected in purified clones but be detected in a population due to its low frequency or due their presence at different sites in the infected organ. In both cases variability in resistance is present in the sampled population but may be not seen when pure clones are analysed. As it has been described for *Mycobacterium tuberculosis* and *Helicobacter pylori* (Zheng *et al.*, 2015; Mascellino *et al.*, 2017; Andersson, Nicoloff and Hjort, 2019), where the heteroresistance phenotype can often be explained though antimicrobial susceptibility tests (AST) methods, diagnose directly on multiple stomach biopsy samples, and sputum samples, without a single colony purification step (Andersson, Nicoloff and Hjort, 2019). Regarding the diagnosis, sampling and analysis of polyclonal heteroresistance may be a problem in some species due to mixed populations containing small resistant subpopulations (Colman *et al.*, 2015; Sun *et al.*, 2018). Alternatively, monoclonal heteroresistance refers to when a single clone, that went through a single cell bottleneck, differentiates into two or more populations at high frequencies detectable when pure clones are analysed. Here, either physiological or genetic heterogeneity could result in heteroresistance phenotype (Andersson, Nicoloff and Hjort, 2019).

Another important factor in heteroresistance is its stability, which can be compromised when cost-effectiveness no longer benefits cell fitness. Unstable heteroresistance can be observed when a resistant clone isolated from the resistant subpopulation generates a mixed population of susceptible and resistant cells when grown in the absence of antibiotics due to the reversibility of the resistance phenotype (Andersson, Nicoloff and Hjort, 2019). For example, one phenomenon that can lead to this phenotype is when genetically stable mutations resulting in resistance (such as insertions, deletions, and SNPs) have a high fitness cost. Here, selection of compensatory mutations can occur that will simultaneously reduce the cost and result in loss of resistance, when grown in the absence of antibiotic pressure (Lee *et al.*, 2011; Hjort, Nicoloff and Andersson, 2016; Nicoloff *et al.*, 2019). Likewise, intrinsically unstable and costly tandem gene amplifications, which result in an increase in the copy number of resistance conferring genes, are lost in the absence of antibiotic selection (Plipat *et al.*, 2005; Hjort, Nicoloff and Andersson, 2016; Andersson, Nicoloff and Hjort, 2019; Nicoloff *et al.*, 2019). On the other hand, when mutations like SNPs, frameshifts, insertions and deletions, have a low

or marginal impact on the fitness of the mutants, the resistance phenotype does not rapidly revert to the susceptible phenotype in the absence of antibiotic selective pressure, and are more likely to establish a stable heteroresistance phenotype (Andersson, Nicoloff and Hjort, 2019; Pereira *et al.*, 2021).

1.5.2. Colistin heteroresistance

Heteroresistance driven by amplification of resistance-associated genes has recently been demonstrated to be the most common type of heteroresistance in Gram-negative bacteria (Hjort, Nicoloff and Andersson, 2016). Regarding the heteroresistance of *A. baumannii* to colistin, subpopulations with high-level of resistance were correlated with loss of LPS production caused by the presence of an insertion sequence in the *lpxA* and *lpxC* genes, resulting in inactivation of the lipid A biosynthesis (Moffatt *et al.*, 2010, 2011; El-Halfawy and Valvano, 2015). Also, increased expression of efflux pumps has been described as a mechanism of resistance in *A. baumannii* subpopulations with stable heteroresistance towards colistin (Machado *et al.*, 2018; Andersson, Nicoloff and Hjort, 2019). Being an underestimated phenomenon in both diagnosis and treatment of infectious diseases, further studies on heteroresistance are needed to answer the question of whether this poses a threat of resistance in clinical practice when using colistin (Pournaras *et al.*, 2005; Petrosillo, Ioannidou and Falagas, 2008).

In this work we proposed to study the characteristics and mechanisms underlying heteroresistance in three subpopulations of a carbapenem-producing *A. baumannii* strain with simultaneous resistance to colistin through antimicrobial susceptibility testing, time-kill assays, PCR amplification and sequencing of the described genes responsible for colistin resistance in *A. baumannii*, presence of active efflux systems as well as regarding the existence of synergy between colistin/ethidium bromide and efflux inhibitors, and overexpression of genes encoding efflux pumps in the presence of colistin.

2. Material and Methods

2.1. Material

2.1.1. Biological material

For the development of this work, we studied three variants isolated from a clinical strain of *A. baumannii* with presence of heteroresistance to colistin, identified as Ab10-6 in studies previously developed in this laboratory, and the reference strain ATCC19606^{T} (DSMZ, Germany). The clinical strain of *A. baumannii* identified as Ab10-6 comes from a collection of 72 carbapenem-resistant strains collected during an outbreak in patients with respiratory infections, isolated in a hospital in Lisbon (Rodrigues, 2019). Their identification was performed using the Vitek GNI+ card system (bioMérieux, Marcy l'Étoile, France) and later sent to the Unit of Medical Microbiology of the Institute of Hygiene and Tropical Medicine (IHMT), on agar plates supplemented with 5% blood agar (bioMérieux), and then stored at -80ºC in Mueller-Hinton broth (MHB) supplemented with 10% glycerol. The isolate is referred to throughout this work by the designation of the species *A. baumannii* (Ab), year of isolation 2010 (10), and sequential numerical identification defined for each of the isolates, in this case isolate 6, that is, Ab10-6 corresponds to *A. baumannii* isolated in 2010, isolate number 6. The selection criteria for the three isolated variants of the Ab10-6 strain corresponded to the different colony morphology. The selection of three isolated variants was performed in this study corresponding to the L variant, S variant and XS variant. Selection criteria and procedures are described in section 2.2.2.1.

2.1.2. Other biological material

To determine the molecular weight of the products of the PCR reactions, the molecular weight marker GeneRuler 50bp DNA Ladder (Thermo Scientific) was used.

Table 1. Nucleotide sequences of primers used in molecular typing ERIC-PCR.

"Primers"	Nucleotide sequence (5' → 3')	Fragment (bp)	Reference
ERIC1	ATGTAAGCTCCTGGGGATTCAC	Variable	(Versalovic, Koeuth and Lupski, 1991)
ERIC2	AAGTAAGTGACTGGGGTGAGCG		

Table 2. Nucleotide sequences of primers used in efflux pump amplification.

Efflux pump	Primers	Nucleotide sequence (5' → 3')	Fragment (bp)	Reference
AdeABC	adeB_Fw	TGTGATGCTAGTTGTGCCA	232	(Machado *et al.*, 2018)
	adeB_Rv	TGTCATCAGAATTGGCCGT		
AdeFGH	adeG_Fw	ACTGCAACTTGAAGACCGA	191	
	adeG_Rv	CATCTGTAACAGCAACGCC		
AdeIJK	adeJ_Fw	CTTCCAGCAATGCCTGAAC	153	
	adeJ_Rv	ATTTGGACGCACACCTACA		
AmvA	amvA_Fw	GCTGATTATGGCGGGTTTG	158	
	amvA_Rv	AGACAGCACGAGAAGCAAT		
AbeS	abeS_Fw	GCAACTTCAGCATTAAAAGCAT	159	
	abeS_Rv	AATAATACCTGCGCCTGACC		
AbeM	abeM_Fw	AGCCCAGTTCTTTTCACCA	118	
	abeM_Rv	TATTGCCGCACACCAAGTA		
CraA	craA_Fw	AGGCCAACGTTAACCCAA	175	
	craA_Rv	TCATGGCACTGGGGTTTC		

Fw, forward; Rv, reverse; bp, base pairs.

Table 3. Nucleotide sequences of primers used in genes associated with colistin resistance amplification.

Gene	Primers	Nucleotide sequence (5' → 3')	Fragment (bp)	Reference
pmrA	pmrA_Fw	AGCGAGCCTAGAACATGACA	753	(Machado *et al.*, 2018)
	pmrA_Rv	GGTGCCCCAAATCAGTCG		
pmrB	pmrB-P1_Fw	AACGACTGATTTGGGGCAC	643	
	pmrB-P1_Rv	TGCTTCTGTTCATTTTGCGC		
	pmrB-P2_Fw	GCTTGCGGGCAGTATGTTGC	629	
	pmrB-P2_Rv	GCTTGCGGGCAGTATGTTT		
	pmrB-P3_Fw	ATTTGTGTGGAGCAGTTGGT	601	
	pmrB-P3_Rv	TTTCATGATGGGTTGGGCG		
lpxA	lpxA1_Fw	CGCCATTATTGATCCATCTGC	411	
	lpxA1_ Rv	CCAATATGTACATGTCCAGCG		
	lpxA2_Fw	CCAAGATAGGTAGTCATAACCT	557	
	lpxA2_ Rv	TCCAAAGTCTGAAGAAGCAA		
lpxC	lpxC1_Fw	ACAGCGTACTCTCAATCGTG	508	
	lpxC1_ Rv	TGCAGACTGATACTCTTTGGCA		
	lpxC2_Fw	AAGCAATATTCAGCCCGCAT	610	
	lpxC2_ Rv	CCAAGCTTTACTACGTTTGGC		
lpxD	lpxD1_Fw	AGGTGAGCTAATTGGTGAAGGT	651	
	lpxD1_ Rv	ATAACCCCATCTTCCAAAATTGT		
	lpxD2_Fw	TTGATAGAGGCGCACTTGAT	461	
	lpxD2_Rv	AGGGATGGCAAATTTAGGTGTAGT		

Fw, forward; Rv, reverse; bp, base pairs.

2.1.3. Growth media and solutions

The preparation and composition of the solutions and growth media used are described in Tables 4 to 8. Growth media and solutions were prepared in distilled water and then sterilized in an autoclave at 121ºC for 15 min at 1 bar, when necessary.

Table 4. Growth media composition.

Growth media [1]	Formulations (per litre)
Mueller-Hinton Broth (MHB) [1]	300g of dehydrated beef infusion; 17.5g casein hydrolysate; 1.5 g of starch; 4.347mg Ca^{2+}; 6.206mg Mg^{2+}; pH 7.3 ± 0.1 at 25ºC
Mueller-Hinton Agar (MHA) [1]	300g of dehydrated beef infusion; 17.5g casein hydrolysate; 1.5g of starch; 17g of agar; 4.347mg Ca^{2+}; 6.206mg Mg^{2+}; pH 7.3 ± 0.1 at 25ºC
Levine EMB Agar [2]	10g of meat peptone; 10g of lactose; 2g of dipotassium hydrogen phosphate; 0.4g eosin yellowish; 65.0 mg of methylene blue; 13.5g of agar; pH 7.0 ± 0.2 at 37ºC
MacConkey II Agar [2]	17.0g of pancreatic digest of gelatine; 1.5g of pancreatic digest of casein; 1.5g of peptic digest of animal tissue; 10g of lactose; 1.5g of bile salts; 5.0g of sodium chloride; 0.03g of neutral red; 0.001g of crystal violet; 13.5g of agar; pH 7.1 ± 0.2

(1) Oxoid, (2) Sigma-Aldrich.

Table 5. Composition and preparation of the solutions used.

Solution	Composition and preparation of the stock solution
EDTA 0.5M, pH 8.0 [1]	232.6g of EDTA in 1 litre of distilled water
Tris-HCl 1M, pH 8.0 [1]	121.1g of Tris-base in 1 litre of distilled water
Glicerol 50% (v/v) [1]	Glycerol in sterile distilled water
Glucose 20% (p/v) [1]	20g of glucose in 100 mL of sterile distilled water [3]
Saline 0.85% [2]	0.85g of NaCl in 100 mL of distilled water

(1) Sigma-Aldrich; (2) Panreac, Barcelona, Spain. (3) Filter sterilized solution with 0.22 μm pore diameter PVDF sterile syringe filters from Rotilabo, Spritzenfilter Steril, Karlshure, Germany.

Table 6. Composition and preparation of the buffer solutions used.

Buffer solutions	Composition and preparation of the stock solution
TE buffer	10 mM Tris-HCl [1] 1 M, 1 mM EDTA 0.5 M pH 8.0 in 1 L of distilled water
TAE 50X buffer	242 g of Tris base [1], 57.1 mL of glacial acetic acid [2] and 100 mL of 0.5 M EDTA pH 8.0 in 1 L of distilled water
Sample buffer	0.1 g of bromophenol blue [3] and 16 g of sucrose [4] in 40 mL of sterile distilled water
Phosphate Buffer Saline (PBS) 1X [1]	10 mM phosphate buffer; 2.7 mM KCl; 137 mM NaCl; pH 7.4

(1) Sigma-Aldrich; (2) Panreac; (3) PlusOne, Amersham Pharmacia Biotech, Easton Turnpike, Fairfield; (4) Merck, Darmstadt, Germany. PBS, phosphate buffer saline.

Table 7. Composition and preparation of substrate and efflux inhibitor solutions.

Compound [1]	Composition, preparation, and storage of the stock solution
Ethidium bromide (EtBr)	10 mg/mL in double-distilled water; 4ºC*
Thioridazine (TZ)	10 mg/mL in sterile double-distilled water; -20ºC *

(1) Sigma-Aldrich. * Photosensitive, protected from light.

Table 8. Composition and preparation of the antibiotic solution used.

Antibiotic [1]	Composition and preparation of the working solution
Colistin sulphate (COL)	10 mg/mL in sterile distilled water; -20ºC*
Daptomycin (DAP)	10 mg/mL in sterile distilled water; -20ºC
Amphotericin B (ANF)	10 mg/mL in 10% glucose; -20ºC

(1) Sigma-Aldrich. * Stored in glass tube.

Table 9. Antibiotics, concentrations, and breakpoints used in the Kirby-Bauer antibiotic susceptibility test.

Class	Antibiotic [1]	Concentration (µg)	Breakpoint (mm)		
			S ≥	I	R <
Penicillins	Ampicillin (AMP) [2]	10	17	14-16	13
	Amoxicillin/clavulanic acid (AMC) [2]	30	18	14-17	13
	Piperacillin (PRL)	100	21	18-20	17
	Piperacillin-tazobactam (TZP)	110	21	18-20	17
	Oxacillin (OX) [3]	1	-	-	-
3G Cephalosporins	Ceftazidime (CAZ)	30	18	15-17	14
	Cefotaxime (CTX)	30	23	15-22	14
	Ceftriaxone (CRO)	30	21	14-20	13
4G Cephalosporins	Cefepime (FEP)	30	18	15-17	14
Carbapenems	Imipenem (IPM)	10	22	19-21	18
	Meropenem (MEM)	10	18	15-17	14
	Doripenem (DOR)	10	18	15-17	14
Aminoglycosides	Amikacin (AK)	30	17	15-16	14
	Gentamicin (CN)	10	15	13-14	12
	Netilmicin (NET) [4]	10	16	-	16
	Tobramycin (TOB)	10	15	13-14	12
Tetracyclines	Doxycycline (DO)	30	13	10-12	9
	Minocycline (MH)	30	16	13-15	12
	Tetracycline (TE)	30	15	12-14	11
Glycylcyclines	Tigecycline (TGC) [5]	15	19	15-18	14
Fluoroquinolones	Levofloxacin (LEV)	5	17	14-16	13
	Ciprofloxacin (CIP)	5	21	16-20	15
Folate pathway inhibitors	Trimethoprim-sulfamethoxazole (SXT)	1.25/23.75	16	11-15	10

(1) Oxoid. R, resistant; I, susceptible, increased exposure; S, susceptible. Antibiotic abbreviations are shown as inscription on the respective discs. (2) Breakpoints for *Acinetobacter* spp. not defined, interpretation based on breakpoints for *Enterobacteriaceae* according to CLSI guidelines (CLSI, 2018). (3) There are no breakpoints for oxacillin for *Acinetobacter* spp. (4) "Breakpoints" according to EUCAST

standards (EUCAST, 2017). (5) Zone diameters interpretation based on the US Food and Drug Administration breakpoints for susceptibility (Pharmaceutics, 2005).

2.2. Methods

2.2.1. Growth and maintenance of bacterial strains

For bacterial growth of the L, S, XS variants, of the clinical isolate Ab10-6 and of the reference strain ATCC19606^T, MHA medium was used with subsequent incubation at 37ºC for 20-24h. These cultures will be referred throughout the work as primary cultures, and overnight cultures refer to the cell growth in Mueller-Hinton Broth (MHB) medium, for 20-24h at 37ºC, with agitation at 180 rpm (Thermo Scientific MaxQ 4000 Benchtop Orbital Shakers, Waltham, MA, USA). The stock solutions of these cultures were kept in liquid medium supplemented with 10% (v/v) glycerol and stored at -80ºC (long-term storage) and -20ºC (short-term storage).

2.2.2. Morphological characterization

2.2.2.1. Morphological characterization by the Levine-agar method

SuperPolymyxin Medium is a selective culture medium developed for the early detection and isolation of Gram-negative bacteria that present reduced susceptibility to polymyxins. The great advantage of this medium is the ability to screen isolates with resistance to polymyxins, being also selective for Gram-negative bacteria and indicative of whether the bacteria are fermenters (blue-red colonies) or not (lavender, colourless or clear) of lactose due to the presence of eosin methylene blue in its composition. Moreover, these medium has been specially designed to prevent contamination with *Proteus* spp., Gram-positive bacteria, and fungi (Nordmann, Jayol and Poirel, 2016). For this work, a selective culture medium was prepared based on the medium developed by Nordmann, Jayol and Poirel (Nordmann, Jayol and Poirel, 2016), as described in Table 10.

Table 10. Preparation of SuperPolymyxin culture medium.

Reagent	Stock solution	Quantities to add	Final concentration
Levine EMB Agar	-	7.5 g	1.9%
Colistin sulphate	20 mg/mL	140 µL	3.5 µg/mL
Daptomycin	20 mg/mL	400 µL	10 µg/mL
Amphotericin B	20 mg/mL	200 µL	5 µg/mL
Distilled water	-	Until 400 mL	-

The different steps of the procedure are exemplified in Figure 1. From an overnight culture grown in 10 mL of MHB, 10-fold serial dilutions were performed using MHB, with subsequent inoculation of 100 µL in the respective plates and incubated at 37ºC for 20-24h. Plates showing isolated colonies were chosen for morphological characterization, and colistin-resistant *Klebsiella pneumoniae* FF61198 strain was used as a positive control (Machado *et al.*, 2018).

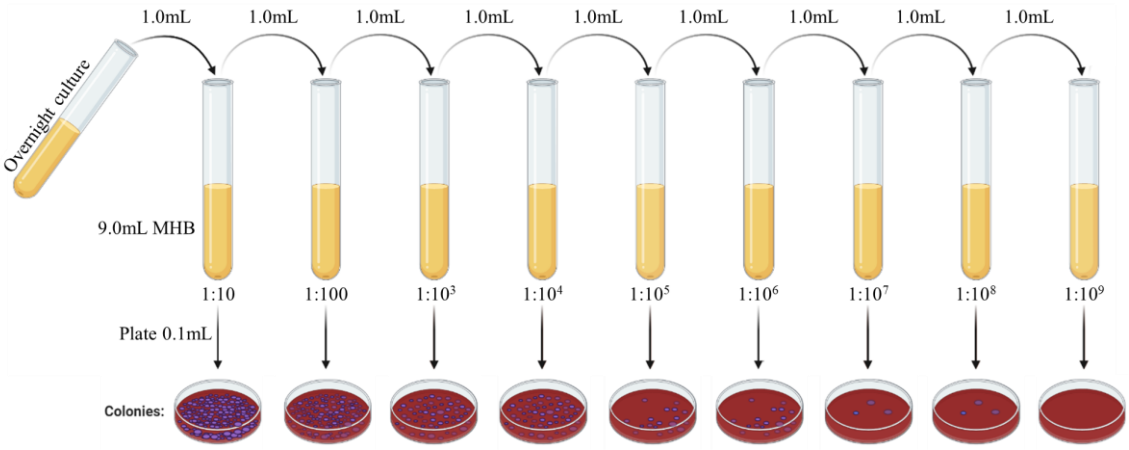

Figure 1. Schematic representation of the preparation of strain suspensions and inoculation in SuperPolymyxin selective medium used for the morphological characterization of the strains under study.

2.2.3. Phenotypic characterization

2.2.3.1. Kirby-Bauer antibiotic susceptibility test (AST)

To help physicians select treatment options for their patients, it is important to determine the sensitivity or resistance of aerobic pathogens and facultative anaerobic bacteria to various antimicrobial compounds. For this purpose, there is the Kirby-Bauer disk diffusion susceptibility test where the pathogen organism is grown on MHA in the presence of several discs of antimicrobial-impregnated filter paper. The presence or absence of growth around the discs is an indirect measure of the ability of that compound to inhibit the growth of that organism (Hudzicki, 2009).

The agar plate is inoculated with a cell suspension with a concentration equivalent to 0.5 on the McFarland scale prepared in 0.85% sterile saline before placing the discs on the agar surface, growth of the bacteria and diffusion of the antimicrobial compounds occurs simultaneously. A 6 mm filter paper disc impregnated with a known concentration of an

antimicrobial compound (see Table 9, section 2.1.3.), is placed on an MHA plate, and diffusion occurs immediately when water from the agar is absorbed by the disc, resulting in antimicrobial diffusion into the surrounding agar. The rate of diffusion through the agar is not as rapid as the rate of extraction of the antimicrobial out of the disc, so the antimicrobial concentration is highest closest to the disc and a logarithmic reduction in concentration occurs as the distance from the disc increases. The rate of diffusion of the antimicrobial through the agar depends on the diffusion and solubility properties of the drug in MHA and the molecular weight of the antimicrobial compound, causing each antimicrobial to have a unique break zone size (Hudzicki, 2009).

Bacterial growth occurs in the presence of an antimicrobial compound when the bacteria can dominate the inhibitory effects of the antimicrobial compound. The agar plate containing the antimicrobial compound and the inoculum is then incubated at 37ºC during 20-24h in the case of *A. baumannii*. The size of the growth inhibition zone is demonstrated by a strong marginal circle of bacterial growth around the disc. The interpretation of resistance and susceptibility has been standardised, and the guidelines can be found in Clinical Laboratory Institute Performance Standards for Antimicrobial Disk Susceptibility Testing (CLSI, 2020).

2.2.3.2. Colistin susceptibility testing by Etest

Etest ("Epsilon Test") is a quantitative diffusion method used for antibiotic susceptibility determination. It consists of thin plastic test strip impregnated with increasing antibiotic concentration gradient (ranging from 0.016 to 256 g/mL). After its placement on the inoculated agar plate (MHA) the antibiotic contained within the strip diffuses into the culture medium creating an ellipse-shaped zone of inhibition. The bacterial inoculum was prepared for a final turbidity equivalent to 0.5 on the McFarland scale, in sterile 0.85% NaCl solution, corresponding to approximately 10^8 CFU/mL, and applied onto the entire surface of an MHA plate through use of a sterile cotton swab by spreading the inoculum in tight streaks. After incubation at 37ºC, for 20-24h the value of the minimum inhibitory concentration (MIC) value was recorded. The MIC is determined by the line of intersection of the bacterial growth with the respective strip (Rodrigues, 2014). The size of the diameter of the inhibition ellipse varies according to the height of the agar, the pH of the medium and other biophysical variables, making it important to rigorously

standardise the preparation of the culture medium according to the reference protocol and the recommendations of the "European Committee of Antibiotic Susceptibility Testing" (EUCAST, 2020). Although microdilution is the reference method recommended by EUCAST to determine colistin susceptibility, in this study we chose to use the Etest method for rapid screening of colistin resistance, as it is the method routinely used in hospital laboratories to screen for resistance to this antibiotic and the only method available for phenotypic detection of heteroresistance to this antibiotic.

2.2.3.3. Determination of minimum inhibitory concentrations (MIC) by the 96-well microplate dilution method

The MIC is defined as the minimum concentration of a given compound necessary to inhibit the visible growth of a microorganism. The MIC can be determined by agar dilution, concentration gradient diffusion, serial microdilution in a 96-well plate and by macrodilution (Wiegand, Hilpert and Hancock, 2008). In this work, MIC were determined by serial microdilution in a 96-well plate.

2.2.3.3.1. MIC determination for colistin, efflux inhibitor and EtBr by the serial microdilution method in a 96-well microplate

Colistin (COL, antibiotic), thioridazine (TZ, efflux inhibitor), and ethidium bromide (EtBr, efflux pump substrate) MIC were performed by serial 1:2 microdilution in 96-well plate, according to the EUCAST recommendations (EUCAST, 2020). The concentration spectrum used was selected based on results previously obtained in the working group and are described in Table 11 (Machado *et al.*, 2018). 96-well plates were prepared as shown in Figure 2.

Table 11. Concentration range used in the determination of MIC through the serial microdilution method in a 96-well microplate.

Compound	Concentration range (µg/mL)
Antibiotic	
Colistin	2 – 1024
Efflux inhibitor	
Thioridazine	0.5 – 256
Efflux substrate	
Ethidium bromide	1 – 512

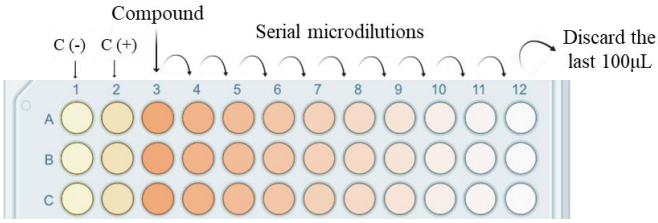

Figure 2. Schematic representation of MIC determination by the serial microdilution method in a 96-well microplate. Compound, colistin, thioridazine and ethidium bromide; C (-), negative control; C (+), positive control.

To all wells of the plate an initial 100 µL of MHB medium was added, except for the first column to which an extra 100 µL of MHB corresponding to the negative control (sterile control) was added. In the third column, 100 µL of the compound solution to be tested was added, prepared 4x more concentrated than the highest desired concentration, followed by a serial dilution of 1:2, where 100 µL from the wells of column 3 were withdrawn to the wells of column 4, and so on, up to column 12, discarding the remaining 100 µL of column 12. Finally, 100 µL of cell suspension, previously adjusted to a concentration equivalent to 0.5 on the McFarland scale, was added starting from column 2, corresponding to positive control (growth control), up to column 12. At the end, each well had a total volume of 200 µL. Results were read visually after an incubation period of 20-24 h at 37°C. Assays were performed in triplicate and those showed growth in the positive control well and no growth in the negative control well were considered valid. The MIC value is considered the result of at least two concordant values.

2.2.3.3.2. Checkerboard assay to determination of COL and EtBr MIC in the presence of TZ, by the serial microdilution method in a 96-well microplate

For the determination of COL and EtBr MIC in the presence of TZ, the assays were performed according to the procedure described in section 2.2.3.3.1., except that prior to the addition of the inoculum, 10 µL of efflux inhibitor TZ was added to all wells from column 3 up to column 12. Thioridazine was tested at subinhibitory concentrations from 0.7 µM to 22.5 µM, to not compromise the cell membrane permeability and viability (Machado *et al.*, 2018). To assess the effect of the efflux inhibitor on the MIC of the antibiotic and EtBr, the modulation factor (MF) was determined (Gröblacher, Kunert and Bucar, 2012) according to the following formula:

$$MF = \frac{MIC\ antibiotic}{MIC\ in\ combination}$$

A decrease of at least ¼ of the MIC value of colistin or EtBr in the presence of the efflux inhibitor was considered as significant (DeMarco *et al.*, 2007).

2.2.3.3.3. MIC determination for colistin, thioridazine and EtBr by the macrodilution method in test tubes

A cell density of 1×10^5 cells/mL was obtained from the dilution of overnight cultures in MHB, and 500 µL of this cell suspension were added to test tubes containing 10 mL MHB and colistin in a range concentration described in Table 12. MIC concentration were read visually after an incubation period of 20-24h at 37°C, with agitation at 180 rpm (Thermo Scientific MaxQ 4000 Benchtop Orbital Shakers, Waltham, MA, USA). A positive control was included in the assay, with drug-free MHB medium, to monitor the normal growth of the strain.

Table 12. Colistin range concentration used in the determination of MIC through the macrodilution method.

Strain/variant	Colistin range concentration (µg/mL) *
Variant L	128-2
Variant S	2048-64
Variant XS	1024-64
Ab10-6	1024-64
ATCC	4-0.0625

*Colistin range concentration based on MIC obtained by the 96-well microplate dilution method according to the CLSI recommendations.

2.2.3.4. Bacterial growth curve

The determination of a cell concentration by assessing the turbidity of a microbial culture in liquid growth medium over time is a quick method that allows experimental acquirement of growth curves by calculating the specific growth rate under certain growth conditions to be tested (Brooks *et al.*, 2012). Thus, for the measurement of the bacterial growth curve in this project, overnight bacterial cultures were adjusted in a test tube containing MHB, at an optical density of 0.6, at a wavelength of 600nm (OD_{600nm}), and subsequently diluted in MHB to a cell density of 1×10^5 cells/mL. Cultures were grown in a fixed volume of 10 mL MHB at 37°C, with agitation at 180 rpm for a period of 24h.

Cell OD_{600nm} measurements were performed every 60min during the first 8h and at 24h on spectrophotometer (Spectronic 200, Thermo Scientific). Bacterial growth curve results from the ratio of cell OD_{600nm} over time.

2.2.3.5. Time-kill kinetic assay

The study of the activity of an antimicrobial agent against a bacterial strain can be carried out through a time-kill kinetic assay, where the bactericidal or bacteriostatic activity of an agent can be determined over time. For the time kill assay bacterial cultures with a cell density of 1×10^5 cells/mL (prepared as described above for bacterial growth curve, section 2.2.3.4.), where grown in the presence of colistin at ¼ of the MIC, with and without 22.5 μM thioridazine as efflux inhibitor. Cultures were grown in a fixed volume of 10 mL MHB at 37°C, with agitation at 180 rpm for a period of 24h. Cell OD_{600nm} measurements were performed every 60min during the first 1-8h and at 24h on spectrophotometer (Spectronic 200, Thermo Scientific). The ratio of cells OD_{600nm} measurement over time results in a death curve. To monitor the normal growth of the strain, a positive control was included for each assay.

2.2.3.6. Ethidium bromide accumulation assay

The semi-automatic fluorometric assay using ethidium bromide (EtBr) is a well-established method for monitoring efflux activities in bacteria (Viveiros *et al.*, 2010). EtBr is a compound that enters the bacterial cell by passive diffusion and because it is a substrate of several efflux pumps, it undergoes cell extrusion via efflux (Paixão *et al.*, 2009; Richmond, Chua and Piddock, 2013). Furthermore, EtBr is a DNA intercalation dye, meaning, its fluorescence increases when intercalated with DNA, providing a way of distinguishing between the intracellular and extracellular localised compound (Richmond, Chua and Piddock, 2013), allowing studies of EtBr accumulation and efflux (Paixão *et al.*, 2009). Thus, the semi-automatic fluorometric assay allows accurate real-time monitoring analysis of the entry and extrusion of EtBr as a substrate for efflux pumps, with the main advantage of simultaneously analyse a large number of samples, the same cell preparation can be exposed to different experimental conditions, and the possible use of reduced volumes of cell suspension and efflux inhibitors (Viveiros *et al.*, 2008; Paixão *et al.*, 2009). To evaluate the efflux activity two types of assays were

performed, primary an assay where EtBr accumulation was determined, and secondly an assay measuring the EtBr efflux as described below.

2.2.3.6.1. Cultures preparation

Three to four colonies of the primary cultures were inoculated into 10 mL of MHB and grown at 37°C, 180 rpm, until an OD_{600nm} of 0.6, corresponding to the exponential growth phase, measured in a test tube spectrophotometer (Spectronic 200, Thermo Scientific). The cultures where then centrifuged at 4000 rpm (Eppendorf 5810R, Hamburg, Germany), for 3 min at room temperature, the supernatant discarded, and the pellet resuspended in 5 mL PBS. According to the requirements for each assay described in the next section, the OD_{600nm} of the suspension was adjusted in a test tube with PBS.

2.2.3.6.2. Accumulation assay

Due to the toxicity of EtBr, it is first necessary to perform an EtBr accumulation assay, without inhibitors, to establish the concentration at which the amount of EtBr entering the cells is equal to the amount leaving the cell per unit of time, establishing equilibrium in the transport kinetics, and corresponding, therefore, to the equilibrium concentration of EtBr for the strains under study. For this protocol, in order to calibrate the EtBr fluorescence reading window according to the sensitivity of the fluorimeter, and the naturally influx and efflux behaviour, it was stipulated that equilibrium concentration of EtBr corresponds to the concentration just below the 10% of relative fluorescence units 10 fluorescence units during the 30 min of the assay (Machado *et al.*, 2017).

EtBr accumulation assays were performed in 96-well round-bottom black plates (ThermoFisher Scientific) with a final volume of 200 µL. The cell suspension was adjusted to an OD_{600nm} of 0.6 with PBS. 100 µL of PBS was added to each well, except for wells in column 1, row G and H. In column 1, 170 µL of PBS was added to wells in rows A to C (glucose free assay) and 166 µL of PBS was added to wells in rows D to F (assay with glucose). Next, 30 µL of an EtBr solution prepared to a final assay concentration of 256 µg/mL was added. This column contains the highest concentration of EtBr, from which serial dilutions by a factor of 2 up to and including column 12 were completed. At column 12, the remaining 100 µL were discarded. In the end, a range of EtBr concentrations of 256 µg/mL down to 0.125 µg/mL was obtained, as represented in

Figure 3. Next, 4 µL of a 20% glucose solution was added to wells in rows D to F, of all columns, obtaining a final assay concentration of 0.4% (v/v) glucose (energy source). Finally, 100 µL of the cell suspension was added to the test plate from column 1 to column 12, row A to row F.

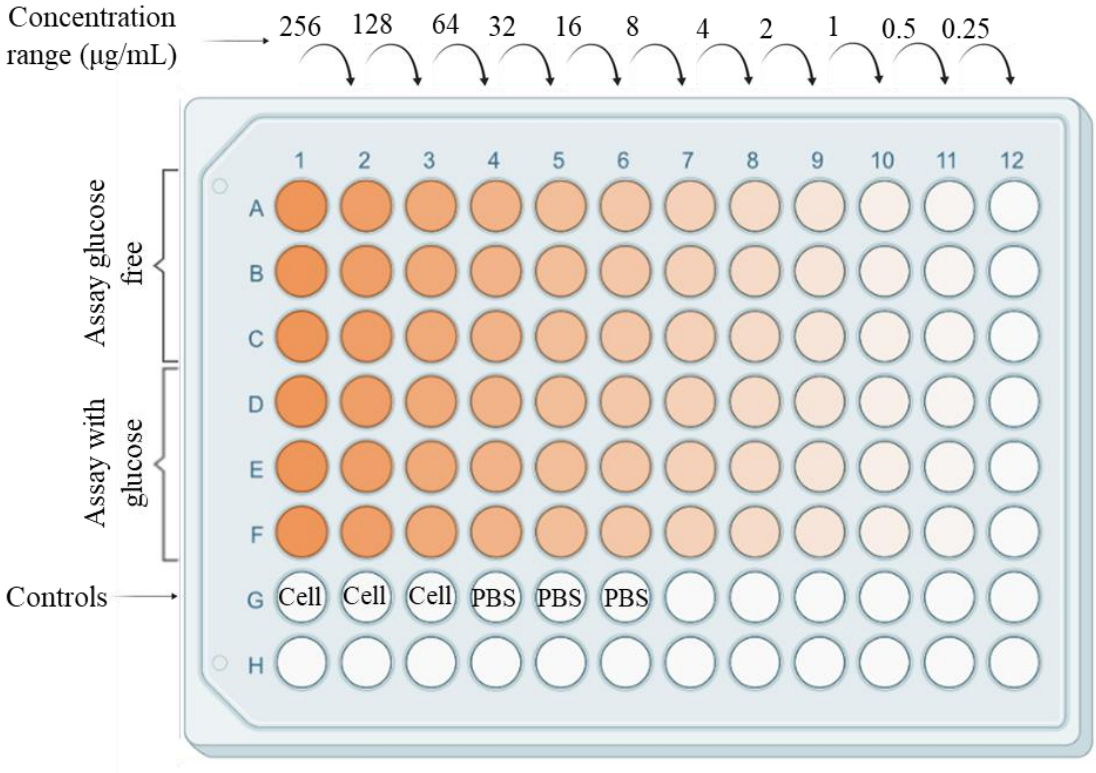

Figure 3. Schematic representation of the 96-well plate preparation used for the ethidium bromide (EtBr) accumulation assays. Indication of the EtBr concentration gradient and the respective columns used. Lines A to C correspond to assay performed in the presence of 0.4% glucose, and lines D to F without glucose. Positive control line G, column 1 to 3 (PBS plus cell), and negative control line G, column 4 to 6 (PBS only) are also distinguished.

A positive control was performed in row G, column 1 to 3, with PBS plus cell, and a negative control in row G, well 4 to 6 just with PBS. The positive and negative controls were used to control the effect of cell and PBS on EtBr accumulation (no accumulation). The 96-well plates were placed in the Synergy HT Microplate Reader and the assays were performed at 37°C. EtBr fluorescence was read at 530/25 and 590/35 nm (Paixão *et al.*, 2009) at every 60 sec cycles for 30 min. The assays were performed in triplicate and biological duplicates.

Once the corresponding equilibrium concentration of EtBr of each strain is established, the EtBr accumulation assays are performed in the presence of the efflux inhibitor. In order to study the influence and efficacy of this compound on the EtBr efflux activity in different strains (Machado *et al.*, 2017).

2.2.3.6.3. EtBr accumulation assay in the presence of efflux inhibitors

To assess the effect of efflux inhibitor on EtBr efflux activity, the cell suspension was adjusted to an OD_{600nm} of 0.6 with PBS, and each strain was tested in the presence of EtBr at the respective equilibrium concentration determined in section 2.2.3.6.2. The activity of the efflux inhibitor thioridazine was evaluated at a concentration of 22.5 μM so that it does not interfere with cell permeability and viability (non-inhibitory concentrations below MIC) (Machado *et al.*, 2017). The 96-well round-bottom black plates (ThermoFisher Scientific) were placed in the Synergy HT Microplate Reader and the assays were performed at 37°C. EtBr fluorescence reading was acquired at 530/25 and 590/35 nm after each 60 second cycle for 30 min. Assays were performed in experimental triplicates and biological duplicates. From the fluorescence values obtained at the end of the 30 min assay, the relative final fluorescence (RFF) was calculated for each strain and the efflux inhibitor (Machado *et al.*, 2011), according to the following formula according to the following formula:

$$RFF = \frac{\mathrm{RF30\,min\ \ (treated)} - \mathrm{RF30\,min(untreated)}}{\mathrm{RF30\,min\ \ (untreated)}}$$

In this formula, RF (treated) corresponds to the relative fluorescence value at the end of the accumulation curve (30 min) in the presence of the efflux inhibitor, and RF (untreated) corresponds to the relative fluorescence at the last point of the accumulation curve (30 min) in the absence of the efflux inhibitor. RFF measures the ability of the efflux inhibitor to provide retention of EtBr within the cell (Machado *et al.*, 2011). Lastly, the arithmetic mean of three independent assays (± standard deviation) of the efflux inhibitor was calculated, and RFF values equal to or greater than 1, were considered as significant inhibitory effect (Machado *et al.*, 2017).

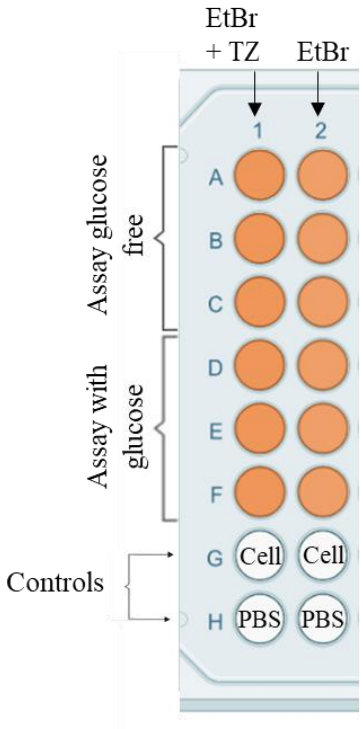

Figure 4. Schematic representation of the 96-well plate preparation used to perform the ethidium bromide (EtBr) accumulation efflux assay in the presence of the efflux inhibitor thioridazine (TZ). Column indication for the position of TZ efflux inhibitor plus EtBr (column 1) and assay in the presence of EtBr only (column 2). Lines A to C correspond to the assay performed in the presence of 0.4% glucose and lines D to F without glucose. Line G, column 1 and 2 corresponds to the positive control (PBS plus cells) and line H, column 1 and 2 to the negative control (PBS only).

In columns 1 and 2, 70 µL of PBS was added to the wells in rows A to C (glucose free assay), and 66 µL of PBS plus glucose at a final concentration of 0.4 % was added to the wells in rows D to F (assay in the presence of glucose), followed by EtBr added so that the final concentration corresponds to the equilibrium concentration as determined in the section above (2.2.3.6.2.), by the EtBr accumulation assay. At last, the efflux inhibitor TZ was added to the wells of columns 1, rows A to F, as exemplified in Figure 4, prepared for a final well concentration of 22.5 µM. Cell suspension was added last to all wells in columns 1 and 2, rows A to F, and negative controls were conducted in row G, column 1 and 2, with PBS plus cell, and a second negative control in row H also in column 1 and 2 with PBS only.

2.2.3.6.4. Ethidium bromide efflux assay

Through this assay, direct overall efflux activity of EtBr can be detected, which can be useful to detect overexpressed efflux activity and interpret different multidrug resistance phenotypes in Gram-negative bacteria (Viveiros *et al.*, 2008; Paixão *et al.*, 2009).

Here maximum EtBr accumulation within bacterial cells was promoted by incubating a cell suspension, with OD_{600nm} adjusted at 0.3, for 1 h at room temperature protected from light, in the presence of EtBr at the equilibrium concentration, and the efflux inhibitor thioridazine at 22.5 µM so that efflux activity is prevented. After 1 h of incubation maximum level of EtBr accumulation is reached (Paixão *et al.*, 2009). Cells were then collected by centrifugation at 13,000 rpm (Biofuge Pico Heraeus Kendro Laboratory Products, Osterode), for 10 min at room temperature and resuspended in EtBr-free PBS until an OD_{600nm} of 0.6.

The cell suspension was then added to previously prepared black 96-well round bottom plates (ThermoFisher Scientific) containing PBS without glucose, PBS with 0.4% (v/v) glucose, PBS with 0.4% (v/v) glucose plus 22.5 µM thioridazine and PBS without glucose with 22.5 µM thioridazine (minimal efflux control), as schematized in Figure 5. EtBr fluorescence was acquired at 530/25 and 590/35 nm at 37°C after each cycle of 60 seconds for 10 min with Synergy HT Microplate Reader. Assays were performed in biological duplicates.

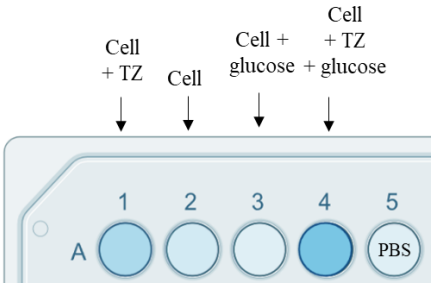

Figure 5. Schematic representation of 96-well plate preparation used in ethidium bromide (EtBr) efflux assay. Column 1 corresponds to the efflux test conditions in the presence of the efflux inhibitor thioridazine (TZ) (Cell + TZ), column 2 corresponds to the efflux-only test conditions of cells in PBS (Cell), column 3 efflux in the presence of glucose as external energy source (Cell + glucose), column 4 corresponds to efflux in the presence of the efflux inhibitor TZ and glucose (Cell + TZ + glucose). A negative control, PBS only, was performed in column 5 (PBS).

Efflux activity was evaluated by quantifying the relative fluorescence value. For this, the data were normalized by comparing the maximum fluorescence where the inhibition of the efflux activity was promoted by the presence of thioridazine obtained from the control cells (fluorescence value corresponding to 1), with the relative fluorescence units produced in the conditions that promote efflux due to the absence of thioridazine and the presence of glucose (Viveiros *et al.,* 2008).

2.2.4. Genotypic characterization

2.2.4.1. Genomic DNA extraction

An adaptation of the "Protocol, Isolation of High Molecular Weight Genomic DNA from *Mycobacteria* (CTAB Procedure)" was performed to obtain high molecular weight genomic DNA for the three variants, Ab10-6 strain and reference strain ATCC19606^{T} (van Soolingen, de Haas and Kremer, 2001).

Thus, 10 mL of overnight culture grown in MHB were centrifuged at 3500 rpm for 16 min at room temperature (Eppendorf Centrifuge 5810R). The pellet was then resuspended in 400 µL of 1x TE and, to promote cell lysis, incubated at 95°C for 20 min with cooling at room temperature. 150 µL of a 10% SDS/proteinase K 10 mg/mL solution was added to each sample, in a proportion of 2:1, with the aim of helping cell lysis by the action of SDS and the degradation of proteins through the cleavage action of proteinase K at the peptide bonds on the carboxylic sides of aliphatic, aromatic, or hydrophobic amino acids, even in the presence of the SDS detergent. After 1h of incubation at 55°C, and before applying 160 µL of CTAB, to remove cell wall debris, denatured proteins and complexed polysaccharides keeping the nucleic acids in solution, it is very important to include 200 µL of 5M NaCl in each sample. This prevents the DNA from binding to cetrimide and prevents the formation of a nucleic acid precipitate in the presence of CTAB if the NaCl concentration drops below 0.5 M at room temperature.

After 10 min of incubation at room temperature, in an equal volume (~1 mL) and at a ratio of 24:1 (v/v), chloroform/isoamyl alcohol was added with subsequent centrifugation at 13000 rpm (Kendro Biofuge Pico Centrifuge D-37520, Osterode) for 5 min. The chloroform/isoamyl alcohol solution precipitates the CTAB-protein/polysaccharide complexes, and a white interface can be observed after centrifugation. This step was

repeated only for the aqueous phase obtained in the first centrifugation, again with the chloroform/isoamyl alcohol solution. In a new eppendorf tube, 560 µL of isopropanol (0.7 vol) were added to the 800 µL of aqueous phase, obtained in the previous step, to obtain the precipitated DNA. After 5 min of incubation and centrifugation at 13000 rpm for 5 min, the pellet was treated with 1 mL of 70% ethanol so that the salts were dissolved, minimizing their solubility, and allowing better precipitation of the DNA in the form of a pellet. Finally, the samples were centrifuged again at 13000 rpm for 10 min at room temperature, with subsequent drying of the pellet in a laminar flow chamber. Before preserving the DNA at -20ºC, it was further hydrated with 50 µL of TE buffer and 5 µL of a 10 mg/mL RNAse solution, to reduce the contamination of the samples with RNA, with overnight incubation. DNA quantification was performed using the Nanodrop 1000 device (Thermo Fisher Scientific).

2.2.4.2. Enterobacterial repetitive intergenic consensus PCR (ERIC-PCR) fingerprinting

Enterobacterial Repetitive Intergenic Consensus (ERIC) PCR is a simple, accurate and cost-effective genotyping technology to discriminate different types of strains (Ranjbar *et al.*, 2017). The ERIC sequence is an imperfect palindrome, found only in intergenic regions, within transcribed regions, and can be found in multiple copies throughout the genome in the form of highly conserved palindromes (Wilson, 2006).

The master mix for ERIC-PCR was performed as follows: 1X Taq DNA polymerase buffer (ThermoFisher Scientific), 1.5 mM $MgCl_2$ (ThermoFisher Scientific), 0.2 mM dNTPs (NZYTech, Portugal), 40 pmol of each primer (primers sequence found in Table 1, section 2.1.2.), 2.5 U Taq DNA polymerase (Thermo Scientific), 100 ng DNA and MiliQ water for a total reaction volume of 50 µL. Handling of DNA, preparation of reaction mixes and processing of PCR products were carried out in separate physical spaces. The PCR reaction was performed in an Eppendorf™ Mastercycler Nexus SX1e, with the following amplification conditions: initial denaturation at 94ºC for 5 min, followed by 35 cycles of denaturation at 94ºC for 1 min, annealing at 52ºC for 1 min and extension at 72ºC for 2 min, with a final extension at 72ºC for 10 min. Samples were kept at 4ºC until further use.

Amplification products were analysed by electrophoresis on a MetaPhor agarose gel at 3% (w/v) (Lonza, Basel, Switzerland). For the preparation of the MetaPhor agarose gel, agarose was dissolved with gentle stirring on a heating plate at 50ºC for around 20 min and then heated at minimum microwave power until complete dissolution. After 30 min of polymerisation at room temperature, the gel was kept at 4°C for a further 45 min. Electrophoresis was performed at 80 V and a current 200 mA for 2 h with 1X TAE buffer at 4ºC on Wide Mini-Sub cell GT system (Bio-Rad) and power supply (Amersham Pharmacia Biotech, Little Chalfont, UK). The gel was stained with 1 µg/mL EtBr for 30 min, after electrophoresis, and the amplification result was visualized under UV light with the Gel Doc XR system (Bio-Rad).

2.2.4.3. PCR amplification of efflux pump-encoding genes

The master mix for the PCR to search for genes encoding efflux pumps was prepared as follows: 1X Taq DNA polymerase buffer (ThermoFisher Scientific), 1.5 mM $MgCl_2$ (ThermoFisher Scientific), 0.2 mM dNTPs (NZYTech), 10 pmol of each primer (primers sequence found in Table 2, section 2.1.2.) and 1 U Taq DNA polymerase (ThermoFisher Scientific), 100 ng DNA and MilliQ water for a total reaction volume of 50 µL. Handling of DNA, preparation of reaction mixes and processing of PCR products were carried out in separate physical spaces. The PCR reaction was performed in an Eppendorf™ Mastercycler Nexus SX1e, with the following amplification conditions: denaturation at 94ºC for 5 min, followed by 30 cycles of denaturation at 94ºC for 30 sec, annealing at 52ºC for 30 sec and extension at 72ºC for 30 sec, with a final extension at 72ºC for 10 min.

The amplification products were analysed by electrophoresis on a 2% (w/v) agarose gel (Sigma) dissolved in 1X TAE buffer also used to run the gel at 120 V and a current of 150 mA for 1 h, with further staining with 1 µg/mL EtBr buffer. The amplification result was visualized under UV light with the GEL DOC XR system (Bio-Rad).

2.2.4.4. PCR amplification and DNA sequencing of genes associated with colistin resistance

Master mix reaction was prepared as follows: 1x NZY Taq II DNA polymerase enzyme buffer (Nzytech), 1.5 mM $MgCl_2$ (Nzytech), 0.2 mM each DNTP (Nzytech), 10 pmol

each primer (primers sequence found in Table 3, section 2.1.2.), 1 U NZY TAQ II DNA polymerase (Nzytech), 100 ng DNA and MilliQ water prepared to a total volume of 50 µL. The PCR reaction was performed with Eppendorf™ Mastercycler Nexus SX1e, with the following amplification conditions: initial denaturation at 94ºC for 5 min, followed by 35 cycles of denaturation at 94ºC for 30 sec, annealing at 52ºC for 30 sec and extension at 72ºC for 30 sec, and a final extension at 72ºC for 10 min. The samples were kept at 4ºC until further use.

Amplification products were analysed by electrophoresis in a 2% (w/v) agarose gel (Sigma) dissolved in 1X TAE buffer which was also used to run the gel at 120 V and 150 mA for 40 min with the Mini Sub Cell GT (Bio-Rad) system and Amersham Pharmacia Biotech EPS 301 power supply, after which was stained with 1 µg/mL of EtBr. The amplification result was visualized under UV light by the GEL DOC XR system (BioRad).

The amplification products were sequenced with same primers used in PCR amplification (primer sequence described in Table 3, section 2.1.2.) (STABVIDA, Caparica, Portugal). The sequences obtained were edited with BioEdit (RRID:SCR_007361) and analysed using the sequence analysis program SnapGene® software (from Insightful Science; available at snapgene.com). Comparison with the sequences of reference strain *A. baumannii* ATCC19606^{T} (GenBank: AP025740.1) was performed using the Clustal Omega program available online at https://www.ebi.ac.uk/Tools/msa/clustalo/ (Sievers *et al.*, 2011).

2.2.4.5. Efflux pump gene expression analysis

2.2.4.5.1. RNA extraction

Total RNA extraction was performed using the RNeasy Mini kit (Qiagen, Hilden, Germany), according to the manufacturer's instructions. In all steps, microtubes free of DNAases and RNAases (Sarstedt, Germany) were used. From an overnight culture grown in 5 mL of MHB, 1 mL was taken and centrifuged at 13000 rpm (Kendro Biofuge Pico Centrifuge D-37520 Osterode) for 10 min. 500 µL of the supernatant was removed and the pellet was resuspended in the remaining volume, to which 1 mL of the "RNAprotect Bacteria Reagent" solution (Qiagen) was later added. The suspension was shaken for 15

sec and incubated at room temperature for 5 min and then centrifuged at 9000 rpm for 10 min. The obtained pellet was resuspended in 100 µL of 1x TE buffer and 3 mg/mL lysozyme (Sigma) was added followed by a 10 min incubation period at room temperature. Next, 350 µL of RLT buffer with 1% β-mercaptoethanol (Sigma) was added and incubated for 15 min at room temperature with a centrifugation at 13000 rpm for 2 min afterwards. Subsequently, the supernatant was transferred to a new sterile microtube, to which 250 µL of absolute ethanol was added, using a micropipette to mix. The solution was transferred to a RNeasy column (Qiagen) and centrifuged at 13000 rpm for 15 sec. Then, 350 µL of RW1 buffer (Qiagen) was added to the column and centrifuged at 13000 rpm for another 15 sec. Two washes were performed with 500 µL of RPE buffer, at 13000 rpm for 15 sec (1st wash) and 2 min (2nd wash). After washing, the column was transferred to a sterile microtube, and RNA was eluted with 80 µL of RNAse-free water (Qiagen) at 13000 rpm for 1 min. Finally, to reduce the presence of contaminating DNA, the samples were treated with DNase I (Qiagen) for 30 minutes at room temperature. The resulting RNA was transferred to a new RNeasy column and centrifuged at 13000 rpm for 15 sec. 350 µL of RW1 buffer (Qiagen) was added to the column and centrifuged at 13000 rpm for 15 sec. Two washes were performed with 500 µL of RPE buffer at 13000 rpm for 15 sec (1st wash) and 2 min (2nd wash). After washing, the column was transferred to a sterile microtube, and RNA was eluted with 80 µL of RNAase-free water (Qiagen) at 13000 rpm for 1 min. Finally, the RNA was stored at -20°C until further use.

2.2.4.5.2. RT-qPCR

The quantification of expression levels of the efflux pump encoding genes was performed by real-time PCR combined with reverse transcription (RT-qPCR). In this technique, a reverse transcription (RT) reaction is performed for the synthesis of cDNA from messenger RNA (mRNA) extracted from the sample under study using the enzyme reverse transcriptase (RT). The synthesized cDNA is amplified by real-time PCR, allowing detection of amplification products as they are amplified (Pfaffl, 2001) due to the incorporation of fluorescent molecules such as SYBR Green I, which is intercalated in the double-strand DNA during amplification reaction (Morrison, Weis and Wittwer, 1998). The quantification of the amplified product is done by monitoring the emitted fluorescent signal which is directly proportional to the amount of DNA amplified in each

cycle (Nolan, Hands and Bustin, 2006). The quantification of gene expression levels can be absolute or relative. In this work, the relative quantification method was used (Livak and Schmittgen, 2001), allowing the relative quantification of the target gene, amplified by comparison with a reference or housekeeping gene. These are genes essential for cell survival whose expression level remains stable regardless of phase and growth conditions (Pfaffl, 2001).

This technique is based on the value of Cq (quantitation cycle) (Bustin *et al.*, 2009), which refers to the cycle number of the amplification reaction. Here the fluorescence signal generated by the amplification of the target molecule crosses the threshold line in the exponential amplification phase of the reaction defined by the detection equipment. The value of Cq is inversely proportional to the amount of cDNA in the sample, which in turn is directly proportional to the amount of mRNA (Bustin, 2000; Schmittgen and Livak, 2008).

For this purpose, One-step RT-PCR was performed (QIAGEN OneStep RT-PCR Kit) using total RNA template (see section 2.2.4.5.1.). These method combines both the reverse transcription (RT) reaction and the polymerase chain reaction (PCR) needed to for the relative quantification of gene expression levels. Here, a single buffer is optimized for both reactions, and the reactions occur in the same tube. Thus, the master mix was prepared as follows, 10 µl of OneStep RT-PCR Master Mix (Qiagen), 10 pmol of each primer (primer sequence described in Table 2, section 2.1.2.), 0.2 µL of OneStep RT-PCR Enzyme Mix (Qiagen), 200 ng RNA and RNase-free water prepared to a total volume of 20 µL. The RT-PCR reaction was performed with the following amplification profile, the Rotor-Gene 3000 real-time thermocycler (Corbett Research, Sydney, Australia) was preheated to 50ºC for 30 sec, followed by an initial cycle of enzymatic activation at 95°C for 15 sec, with 40 subsequent cycles of denaturation at 94°C for 30 seco, annealing at 52°C for 30 sec, extension at 72°C for 30 sec, and a final extension 72°C for 5 min.

Each assay was performed in triplicate, using total RNA obtained from three independent cultures. The formation of non-specific products and primer dimers was evaluated by analysing the melting curves of PCR reactions.

To normalize the results obtained, 16S rRNA was used as a reference gene. The gene expression levels were determined by the comparative or second derivative method, which allows comparing the expression level of two genes, one of them being the chosen reference gene (Livak and Schmittgen, 2001). The expression levels of the genes under study were quantified according to the following formula:

$$\text{Relative gene expression} = 2^{\Delta Cq\text{sample} - \Delta Cq\text{reference}}$$

A relative expression level of 1 indicates that the gene expression level is equal to that of the strain being compared. Overexpression was considered for values equal to or greater than 2. For each gene, the mean ± standard deviation was calculated for the expression levels obtained.

3. Results and discussion

3.1. Morphological characterization of colonies by growth in SuperPolymyxin medium

The parental *A. baumannii* strain Ab10-6, from where the variants were isolated, belongs to ST218, clonal complex (CC)92 and clonal lineage II (GC2) (from global clone), also called international clone II. By searching for mutations in genes associated with colistin resistance (*lpxA*, *lpxB*, *lpxC* and *pmrAB*) by PCR and sequencing the amplified fragments, mutations were identified in this parental strain (Rodrigues, 2019). However, in later studies, Ab10-6 strain was found to show high variability in the levels of susceptibility to colistin when tested by the same method and experimental conditions or by different methods, such as the determination of MIC by microdilution (unpublished data), indicating that the presence of the genetic alterations associated with colistin resistance could not be the only factor responsible for colistin resistance in this strain. Furthermore, it was also verified the presence of colonies with different morphologies in cultures on solid medium, not always evident throughout the work (Gothe, 2020). Therefore, it was hypothesized that this variability in the susceptibility profile presented by the clinical isolates under study could be explained by the phenomenon of heteroresistance, due to the genetic and phenotypic variability in the same population of *A. baumannii* (Li *et al.*, 2006; El-Halfawy and Valvano, 2015; Deveson Lucas *et al.*, 2018; Machado *et al.*, 2018).

Thus, in this work, three variants of the parental Ab10-6 strain were isolated by their growth in Superpolymyxin medium. The selection criteria for the three isolated variants corresponded to the morphological differences presented by the colonies. Thus, the "L" variant was obtained, which presents a morphology of large, rounded colonies, with a dotted and glistening surface, of various shades of purple and mucoid colour, the "S" variant with intermediate size, rounded colonies with purple glistening surface, of turbid purple and mucoid colour, and the "XS" variant contrasting with small, rounded, almost non-pigmented, glistening surface, and dry colonies (Figure 6A).

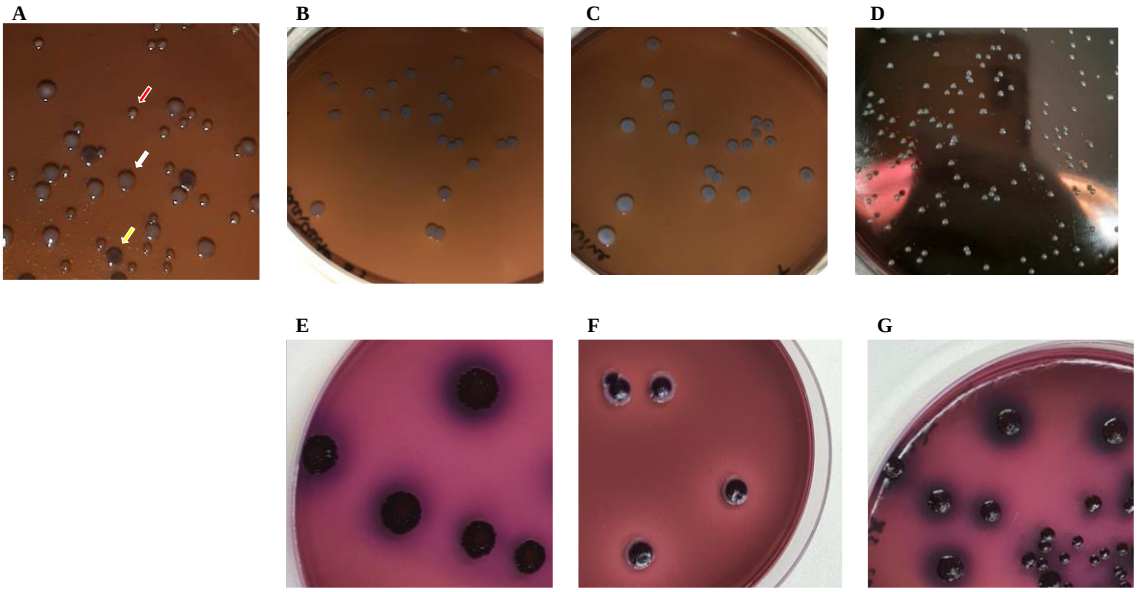

Figure 6. Morphological characterization of colonies by the Levine-agar method in SuperPolymyxin medium. **A**) clinical isolate Ab10-6 at dilution $1:10^7$ and the variants isolated from the strain, **yellow arrow**, L variant; **white arrow**, S variant; **red arrow**, XS variant. **B)** L variant at 24 h at dilution $1:10^7$. **C)** S variant at 24 h at dilution $1:10^7$. **D)** XS variant at 24 h at dilution $1:10^8$. **E)** L variant at 96 h at dilution $1:10^6$. **F)** S variant at 96 h at dilution $1:10^6$. **G)** XS variant at 96 h at dilution $1:10^7$. XS variant results were always analysed at a dilution above due to the reduced visibility of the colonies at bare eye.

After 24 h, the plates were left on the counter for another 72 h to better evaluate the morphology of the colonies. Significant differences in colony morphology were detected when the different variants were compared. The L variant exhibited strongly pigmented colonies of an opaque dark purple, almost black colour, with flat elevation, low glistening, rough and wrinkled surface, with irregular form and undulated margin. The S variant displayed an entire margin and circular form of colony, with a smooth, glistening surface of a convex elevation, and two distinct shades between the opaque dark purple almost black centre with the milky peripherical line. The colonies of the XS variant turned out to be utterly opaque, black pigmented, of a circular form, entire margin, convex elevation, and a rough, glistening, wrinkled surface, along with strong pigmentation of the surrounded medium culture. Colony morphology was analysed according to the characterization criteria presented by the CDC and the Society for Microbiology (Division of Laboratory Systems (DLS), 2020; Society, 2022).

Moreover, all variants presented to be lactose-positive even though, at 24 h, the variant XS appeared to have no dark purple pigmentation (Nordmann, Jayol and Poirel, 2016). A distinct feature was observed regarding the pigmentation of the culture medium. Variants L and XS changed the original homogeneous red pigmentation of the culture medium to now show a gradient that ranges from dark purple near the colonies to a light pink as the distance from the colony increases. This phenomenon could be an extension of the pigmentation due to the fermentation of lactose present in the variants, which is detectable in this culture medium by the presence of methylene blue and eosin in its formula (Levine, 1943).

3.2. Enterobacterial repetitive intergenic consensus PCR (ERIC-PCR) patterns

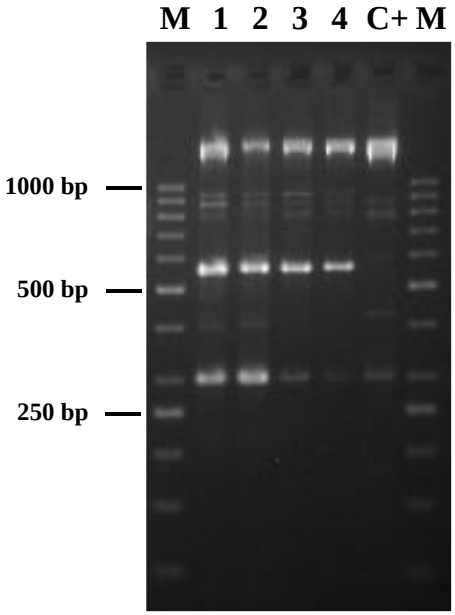

Figure 7. ERIC-PCR profile for each of the three strain variants and the parental strain Ab10-6 of *A. baumannii* clinical isolate. The number indicated above each column corresponds to the identification of each isolate. **M**, Molecular weight marker GeneRuler 50bp DNA Ladder. **1**, variant L. **2**, variant S. **3**, variant XS. **4**, Ab10-6. **C+**, reference strains ATCC19606^T (DSMZ, Germany).

ERIC-PCR analysis confirmed the isogenic nature of the three strain variants. The XS variant is most closely related to the parental strain Ab10-6, as the genetic profile of the bands is the same for both isolates, whereas the L and the S variant show an extra band of ~400 bp (Figure 7.). The one band difference can be explained by insertion or deletion

mutations that result in variability in the number and size of ERIC sequences resulting from the constant evolutionary process (Wilson, 2006).

3.3. Colistin susceptibility testing by Etest

As an alternative to population analysis profile (PAP), the gold standard method, heteroresistance can be detected using Etest. Although the appearance of colonies within the zone of inhibition depends on the frequency of the resistant subpopulation of cells, when heteroresistance is very evident and at a high frequency it is shown to be a rapid and effective method for the detection of heteroresistance (Sherman, Wozniak and Weiss, 2019).

Thus, assessment of colistin susceptibility by the Etest method of the parental strain Ab10-6 showed the growth of small colonies within the zone of inhibition, resulting from the presence of subpopulations with different levels of colistin resistance, being considered heteroresistant to colistin (Figure 8.) (Poirel, Jayol and Nordmann, 2017). When isolated, the three subpopulations exhibit a clear zone of inhibition with no colony growth within it and relatively different MIC levels (Table 13. Section 3.5.).

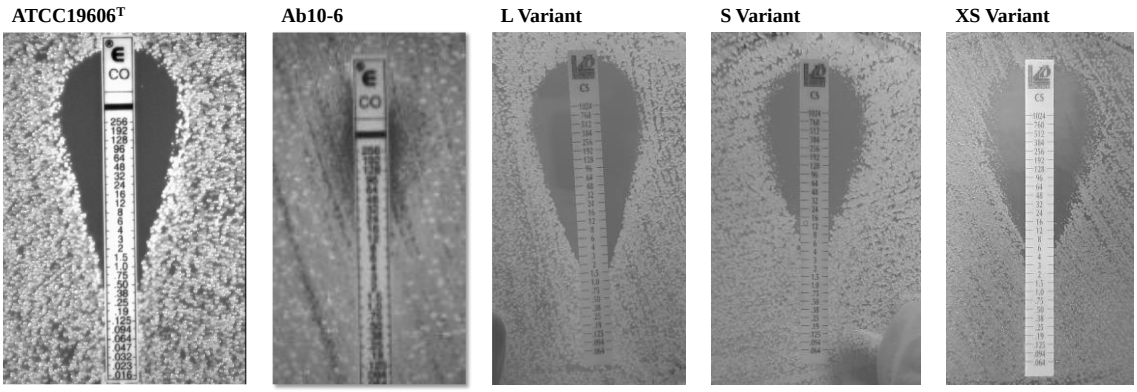

Figure 8. Image showing susceptibility test results obtained by Etest for the clinical strain Ab10-6 and its variants L, S and XS, plus ATCC19606 as a positive control.

3.4. Growth curves of the *A. baumannii* strain variants

The growth rate in the absence of antibiotics was followed over time for the different variants, parental strain Ab10-6, and references strain ATCC19606. The L and S variants show a slower growth rate when compared to the parental strain Ab10-6 and the XS variant which had a growth rate closer to the parental strain. Differences in growth rate

in subpopulations of a strain may have important significance as they may lead to therapeutic failure (Leggett *et al.*, 2017).

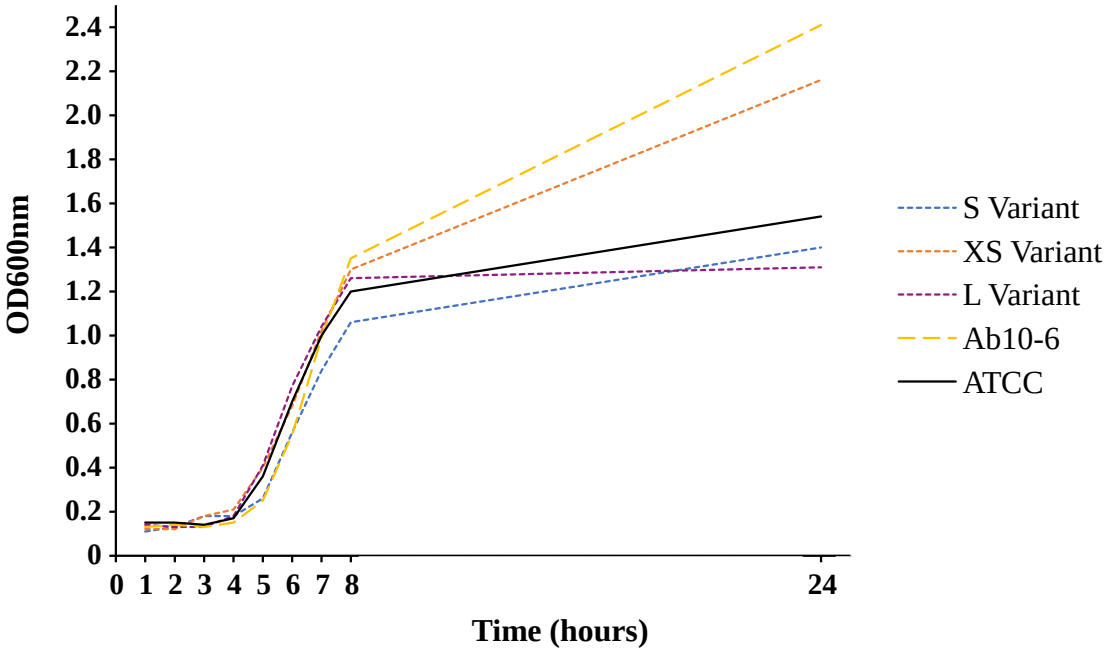

Figure 9. Growth curves of the *A. baumannii* clinical strain Ab10-6, Ab10-6 variants L, S and XS, and reference strain ATCC19606, monitored for 24 h.

When compared to ATCC19606, the growth rate of the parental strain Ab10-6 and the XS variant is much superior, and the ATCC19606 did not reach the same final OD_{600nm} in 24 h as these two variants. The current consensus is that slow cell growth represents a virulence mechanism that may lead to reduced antibiotic efficacy resulting in bacterial survival, but recent studies have shown that fast-growing phenotypic variants may have a lower antibiotic sensitivity due to increased expression and abundance of drug targets and efflux pumps (Łapińska *et al.*, 2022).

3.5. Resistance profile characterization and determination of minimum inhibitory concentration (MIC)

The results of the antibiogram obtained by the Kirby-Bauer disk diffusion method are shown in attachment 1. In previous work, the Ab10-6 strain showed an MDR phenotype with resistance to carbapenems (Rodrigues, 2019). In this study, the same assay was used for isolated subpopulations of the clinical strain Ab10-6 to characterize the resistance

profile and observe if there are differences between the subpopulations when compared with the parental strain. Antibiotic selection was performed based on antibiotics commonly used to treat *A. baumannii* infections and others known to be efflux substrates such as oxacillin. Also, the penicillin class of antibiotics was included as a control for *A. baumannii*, since this species is naturally resistant to them (Jones *et al.*, 2007; Karageorgopoulos and Falagas, 2008; Mendes *et al.*, 2008). The reference strain *A. baumannii* ATCC19606 was used as a control in all assays.

Regarding the fluoroquinolones, glycyclines, aminoglycosides and carbapenems antibiotic classes and folate pathway inhibitor, the results for the parental strain and its derivates showed the same susceptibility levels, all of them being resistant. Differences in susceptibility were observed in the cephalosporin 3rd generation antibiotic class, where both the parental strain Ab10-6 and its variant XS showed an intermediate susceptibility profile as rather than variants S and L, whose susceptibility profile was of resistance. As for cefepime (FEP), an antibiotic belonging to the 4th generation cephalosporin class, changes in resistance profiles were also observed, here all the isolated variants showed an intermediate susceptibility profile while the parental strain demonstrated to be susceptible. Also, regarding the tetracycline class, two of the three antibiotics tested showed different levels of susceptibility between the variants and the parental strain Ab10-6, these showed a resistant and intermediate susceptibility profile to the antibiotic doxycycline, resistant and susceptible to the antibiotic minocycline respectively. Thus, we observed that susceptibility profiles may be diverse between subpopulations of a clinical *A. baumannii* isolate. Results such as these may help understanding the cause of therapeutic failure when resistant subpopulations may be selected under pressure in the presence of a given antibiotic.

Table 13 presents a compilation of the results for the last line antibiotic colistin MIC obtained by the microdilution method in 96-well plates method, macrodilution in test tubes method, and Etest.

Table 13. Colistin minimum inhibitory concentration (MIC) using different methods.

Antibiotic (μg/mL)	*A. baumannii*				
	ATCC19606	Ab10-6	L variant	S variant	XS variant
	Microdilution				
COL	2	128	16	>1024	512
	Macrodilution				
COL	0.25	32	8	128	64
	Etest				
COL	0.75	128	2	16	24

Col, colistin.

One-dilution variations in MIC values were not considered significant as they may be due to the error associated with the technique used to determine the MIC. Thus, significant differences in colistin susceptibility results were observed among the different subpopulations isolated.

S variant presented the highest MIC value of >1024 μg/mL, followed by the XS variant with 512 μg/mL, and L variant with a MIC of 16 μg/mL, 2-fold lower than S variant and 16-fold lower than XS variant, demonstrating the variety of resistance response that can be found among a clinical isolate. Studies indicate that high-level colistin resistance in isolates with MIC > 32 μg/mL is due to the presence of mutations in genes associated with resistance to this antibiotic (Adams *et al.*, 2009; Moffatt *et al.*, 2010; Arroyo *et al.*, 2011; Beceiro *et al.*, 2011). Therefore, a mutation screening was performed for the clinical isolate Ab10-6 and its variants, as described in the section below. Moreover, when analysed by macrodilution and Etest method, all three variants presented different MIC form each other and when compared with the parental strain Ab10-6. The results of the macrodilution showed again that the S variant presented the highest MIC value, followed by the XS variant and, finally, the L variant. However, through the Etest method, the XS variant is the one with the highest MIC value followed of the S and the L variant.

3.6. Chromosomal mutations screening in genes associated with colistin resistance.

The genes selected for mutation screening were *pmrA*, *pmrB*, which encode the two-component PmrAB system, and the genes *lpxA*, *lpxC*, *lpxD* responsible for lipid A biosynthesis, described as genes associated with colistin resistance (Poirel, Jayol and Nordmann, 2017). Results can be found in Table 14.

Table 14. Analysis of chromosomal mutations in genes associated with colistin resistance.

Strain/ variant	MIC colistin (µg/mL)	Gene				
		pmrA	*pmrB*	*lpxA*	*lpxC*	*lpxD*
ATCC19606	0.25	wt	wt	wt	wt	wt
Ab10-6	128	-	L271R N440H	-	N287D	E117K
L Variant	16	-	L271R N440H	-	N287D	E117K
S Variant	>1024	-	L271R N440H	-	N287D	E117K
XS Variant	512	-	L271R N440H	-	N287D	E117K

MIC, minimum inhibitory concentration; -, no mutations were detected; D, aspartic acid; E, glutamic acid; H, histidine; K, lysine; L, leucine; N, asparagine; R, arginine.

Both the clinical strain Ab10-6 and its variants displayed the same result regarding the presence of mutations in the genes that were tested. The genes selected for mutation screening were *pmrA* and *pmrB*, which encode the two-component PmrAB system. The PmrB protein is responsible for the activation of the PmrA protein by phosphorylation, which in turn activates the transcription of the *pmrCAB* operon that is involved in the modification of LPS. Colistin resistance has been associated with specific mutations in the *pmrA* and *pmrB* genes in *K. pneumoniae*, *Enterobacter aerogenes*, *Salmonella enterica* and *A. baumannii*. In *A. baumannii* these mutations result in upregulation of the *pmrCAB* operon and consequently alteration of lipid A and modification of LPS (qualitative modification of LPS) (Poirel, Jayol and Nordmann, 2017). In this study we found a double mutation in the *pmrB* gene (L271R and N440H) in the clinical isolate and all its variants, with no alterations being observed for the *pmrA* gene. Hong, Kim, and Ko also described a mutation on amino acid position 271, but in their case a leucine changed to a phenylalanine (Hong, Kim, and Ko, 2020), whereas in our study an arginine was found in the place of a leucine. Furthermore, the mutation at this position ceased to exist

when the same variant was exposed to increasing levels of colistin, for Hong, Kim, and Ko (Hong, Kim, and Ko, 2020). Despite being present in all variants, no pre-exposure to colistin was conduct for the mutations screening in the present work, which could be an interesting approach for future studies.

In addition, the *lpxA*, *lpxC*, and *lpxD* genes were screen for mutation since they are responsible for lipid A biosynthesis and, when mutated, lead to complete loss of LPS (quantitative LPS modification), being therefore described as genes associated with colistin resistance. Mutations such as truncations, substitutions, and insertion inactivation (by the insertion sequence IS*Aba11*) are among the mutations identified in these genes for *A. baumannii* (Poirel, Jayol and Nordmann, 2017). In this study, *lpxC* and *lpxD* genes yield a single mutation (N287D and E117K, respectively) in the clinical isolate Ab10-6 and all its variants, with no alterations being observed for the *lpxA* gene. To the best of our knowledge, none of the mutation here are described in the literature. The involvement of the present mutations with colistin resistance phenotype cannot be done directly, as complementation or site-directed mutagenesis was not performed, therefore, this should be included in future works to study the contribution of each of the identified polymorphisms in colistin resistance.

3.7. Indirect detection of active efflux systems by checkerboard assays

In addition to porin mutations, overexpression of efflux pump systems is also associated with colistin resistance (Olaitan, Morand and Rolain, 2014; Poirel, Jayol and Nordmann, 2017; Machado *et al.*, 2018). To assess the contribution of efflux activity to colistin resistance in the clinical strain under study and its variants, a checkerboard assays was performed using colistin alone and in combination with the efflux inhibitor TZ. Furthermore, the same assay with EtBr instead of colistin was performed since this compound serves has substrate of most efflux pumps (Paixão *et al.*, 2009; Richmond, Chua and Piddock, 2013).

The minimum inhibitory concentration (MIC) for the efflux substrate ethidium bromide (EtBr) and efflux inhibitor thioridazine (TZ) assessed by the microdilution method in 96-well plates method can be found in Table 15.

Table 15. EtBr and TZ minimum inhibitory concentration (MIC).

Compound	*A. baumannii*				
	ATCC19606	Ab10-6	L variant	S variant	XS variant
	Microdilution				
TZ (μM)	32	64	32	64	64
EtBr (μg/mL)	>256	>256	>256	>256	>256

TZ, thioridazine; EtBr, ethidium bromide.

One-dilution variations in MIC values were not considered significant as they may be due to the error associated with the technique used to determine the MIC. All isolates as well as the reference strain have identical MIC values for the efflux inhibitor TZ, values ranging between 32-64 μM, and EtBr with a constant MIC value of 256 μg/mL, indicating that both EtBr and TZ require high concentrations to exert their antimicrobial activity.

Subsequently, assays of synergism between colistin or EtBr were performed in the presence of increasing concentrations of the efflux inhibitor TZ (see Table 16 and Table 17). The selection of TZ as the efflux inhibitor was based on previous work where it was found to be the most efficient efflux inhibitor in inhibiting efflux activity in *A. baumannii* (Machado *et al.*, 2018). TZ is an inhibitor of calcium channels and inhibits efflux activity indirectly, interrupting cellular energy through inhibition of the electron transport chain. The maximum concentration of TZ tested was 22.5 μM in order not to interfere with cell permeability (Machado *et al.*, 2018).

Table 16. Colistin MIC values in the presence and absence of TZ and modulation factor (MF).

MIC COL (μg/mL) (MF)							
Strain/variant	**COL (μg/mL)**	**With TZ (μM)**					
		22.5	**11.3**	**5.6**	**2.8**	**1.4**	**0.7**
ATCC19606	0.25	**0.0078 (↓≥32x)**	**<0.0078 (↓≥32x)**	**0.0156 (↓16x)**	**0.0312 (↓8x)**	0.125 (↓2x)	0.125 (↓2x)
Ab10-6	128	**32 (↓4x)**	**32 (↓4x)**	64 (↓2x)	64 (↓2x)	64 (↓2x)	64 (↓2x)
L variant	16	16	16	16	32 (↑2x)	**64 (↑4x)**	**64 (↑4x)**
S variant	>1024	128 (↓8x)	128 (↓8x)	128 (↓8x)	128 (↓8x)	512 (↓2x)	>1024
XS variant	512	256 (↓2x)	512	512	512	512	512

MIC, minimum inhibitory concentration; COL, colistin; TZ, thioridazine; MF, modulation factor. In bold are MIC decreases equal to or greater than 4-fold. In red are MIC increases equal to 4-fold.

A variety of responses to the presence of the TZ efflux inhibitor were observed ranging from ≥ 2 - 32-fold reductions in the MIC of colistin to a 4-fold increase in MIC value (antagonism). As for the ATCC19606 strain, TZ produced the strongest inhibition effect, bringing colistin MIC down 32-fold to 0.0078 μg/mL when compared with colistin MIC in the absence of TZ. Regarding the parental clinical strain Ab10-6, a weaker yet significant reduction effect was observed, with the colistin MIC being reduced up to 4-fold. However, variants of the Ab10-6 strain showed significant differences in response to the presence of TZ. While S variant presented a similar response to the parental strain, with a 8-fold colistin MIC reduction, no reduction effect was observed for XS and L variants, indicating that from an indirect point of view the efflux activity does not seem to have a contribution in the mechanisms of resistance to colistin as it has for the S variant and the parental strain. Furthermore, an increase in MIC value for the L variant up to 4-fold was observed when in the presence of a lower concentration of the efflux inhibitor. This phenomenon is described in the literature as an antagonistic response to the presence of more than one antimicrobial compound (Moody, 1992).

Table 17. Ethidium bromide MIC values in the presence and absence of TZ and modulation factor (MF).

MIC EtBr (μg/mL) (MF)							
Strain/variant	**EtBr (μg/mL)**	**With TZ (μM)**					
		22.5	**11.3**	**5.6**	**2.8**	**1.4**	**0.7**
ATCC19606	256	256	256	256	256	256	256
Ab10-6	256	256	256	256	256	256	256
L variant	256	>512	>512	>512	>512	>512	>512
S variant	256	>512	>512	>512	>512	>512	>512
XS variant	256	256	256	256	256	256	256

MIC, minimum inhibitory concentration; EtBr, ethidium bromide; TZ, thioridazine; MF, modulation factor.

No reductions were observed in the MIC values for EtBr in the presence of TZ. The L and S variant presented a MIC increase from 256 μg/mL to >512 μg/mL (512 μg/mL was the maximum concentration used).

3.8. Time kill assay for colistin

To evaluate the effect of colistin on bacterial growth, time kill assays were performed where cells were exposed to half of the colistin MIC and TZ at 22.5 μM. In all variants, as well as for the parental strain, the bacterial growth rate decreased significantly and was completely disrupted in the presence of the efflux inhibitor TZ (see Figure 10). However, the L variant, once again, showed the ability to overcome bactericidal effect of colistin combined with TZ, and was still able to grow presenting the same cell density at 24 hours as for cell density in the presence of colistin alone. Together with the 4-fold increase in colistin MIC observed in checkerboard assays, these results indicate that L variant possesses some resistance mechanism that allows it to overcome antibiotic and efflux inhibitor pressure.

No regrowth was observed as it has been reported for colistin-susceptible *A. baumannii* isolates (Owen *et al.*, 2007), however colistin was very active in the lag phase of the growth curve extending this phase from 4 up to 8 hours after inoculum. Colistin has also been reported to have a greater initial killing rate in *A. baumannii* strains (Owen *et al.*, 2007; Poirel, Jayol and Nordmann, 2017), which could be evaluate through counting of viable cells to search for differences on the effect of colistin in different subpopulations of colistin heteroresistance *A. baumannii* clinical isolate Ab10-6.

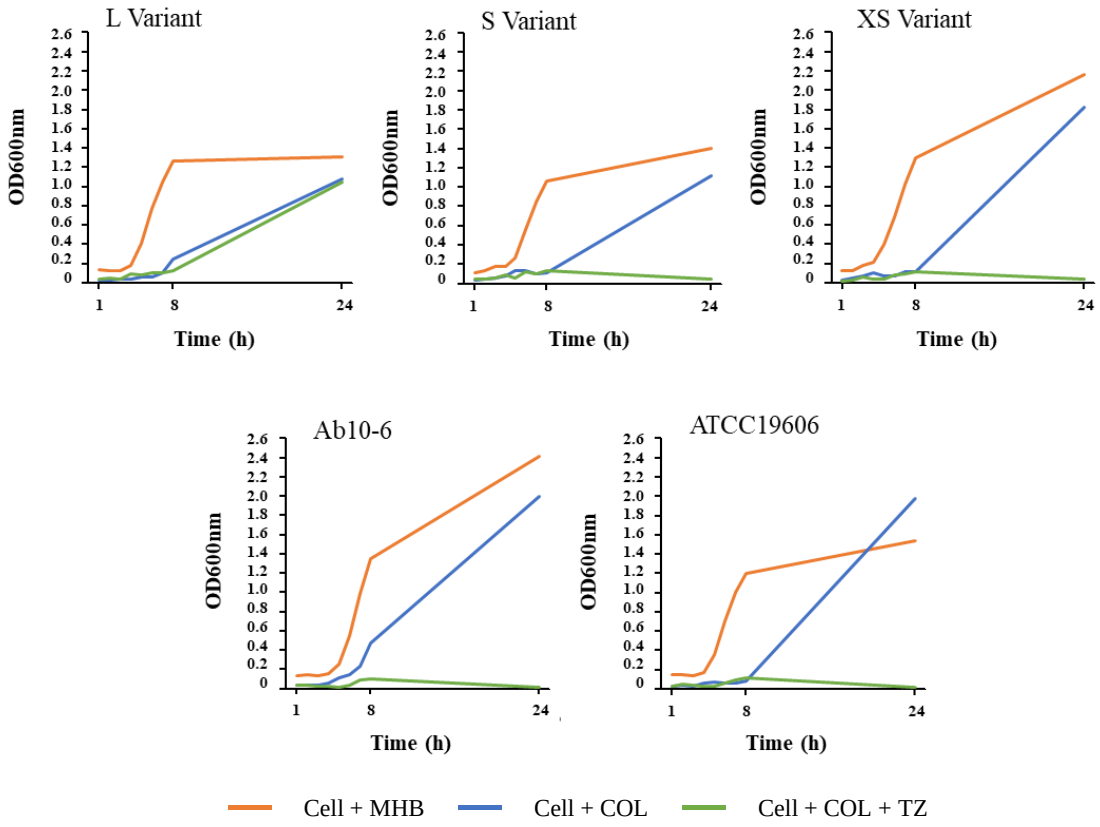

Figure 10. Death curves of the *A. baumannii* clinical strain Ab10-6, Ab10-6 variants L, S and XS, and reference strain ATCC19606, monitored for 24 h. **Cell**, bacterial inoculum; **MHB**, Mueller-Hinton broth; **COL**, antibiotic colistin; **TZ**, efflux inhibitor thioridazine.

3.9. Detection of active efflux systems by the semi-automatic 96-well microplate fluorometric method

To confirm efflux activity, EtBr accumulation assays were performed by the semiautomatic fluorometric method in a 96-well plate with the use of Synergy HT fluorimeter.

The present assay consists of three phases, first it is necessary to acquire the concentration at which the cells accumulate EtBr without impairing cell viability, referred to as equilibrium concentration. Secondly, the accumulation of EtBr inside the cells was promoted by the presence of the TZ efflux inhibitor and finally, the overall efflux activity of EtBr was assessed. In these assays, 0.4% glucose was provided as an external source of energy for the cells, since all efflux pumps capable of extrusion of antibiotics are

energy dependent, such as the RND family efflux pumps, which depends on the proton potential (Paixão *et al.*, 2009; Yoon *et al.*, 2015).

3.9.1. Detection of active efflux systems by the semi-automatic 96-well microplate fluorometric method

To determine the equilibrium concentration of EtBr, an accumulation assay was performed for this compound, in which the isolates and the reference strain under study were exposed to increasing concentrations of EtBr (0.25 to 5 µg/mL). The equilibrium concentration of EtBr was considered as the concentration for which the fluorescence values are just below 10 fluorescence units (Figure 11). At this concentration, it is possible to visualize the effects of EtBr accumulation in cells without jeopardizing cell viability.

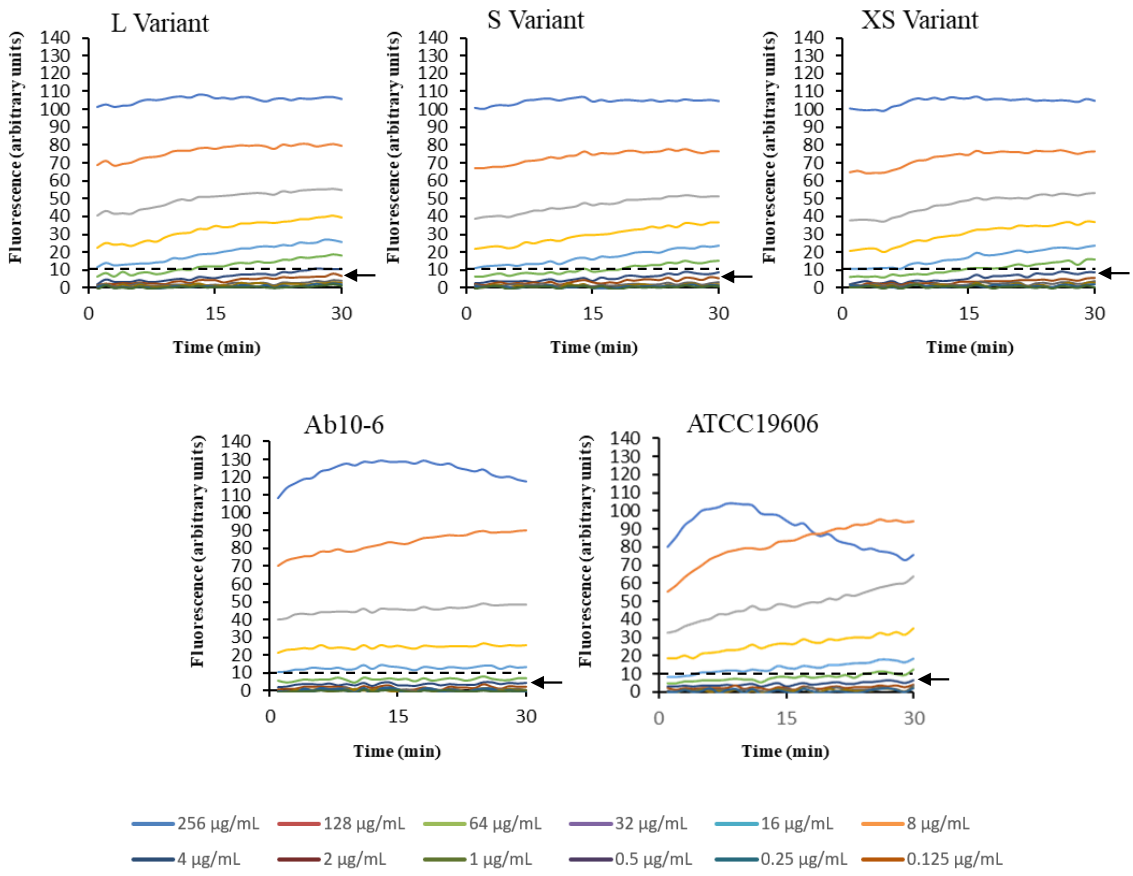

Figure 11. Determination of the equilibrium concentration of EtBr for the clinical strain Ab10-6, its variants and for the reference strain ATCC19606. The arrow indicates the chosen equilibrium concentration for each isolate.

Based on the analysis of Figure 11, the following equilibrium concentrations were determined for the isolates and reference strain: 4 μg/mL for Ab10-6 and XS variant; and 2 μg/ml for the S variant, L variant and ATCC19606.

These results indicate that the Ab10-6 and the XS variant are capable of efflux more EtBr than the reference strain, the S variant, and the L variant. The same assay carried out in the presence of glucose displayed a slight decrease in fluorescence levels since the efflux pumps activity is potentiated by the addition of a source of energy. This will lead to the need for greater concentration of EtBr to reach the equilibrium concentration between the influx and efflux of this substrate and only when this concentration is exceeded, there will be intracellular accumulation of EtBr.

3.9.2. Evaluation of ethidium bromide accumulation in the presence of efflux inhibitor TZ

After the determination of the equilibrium concentrations, the study was continued by evaluating the EtBr efflux capacity of the isolates under study, quantifying the levels of EtBr accumulation in the presence and absence of efflux inhibitor. The results obtained for the isolates under study in the presence of the efflux inhibitor and in the absence of glucose are presented in graphical form in Figure 12, and through RFF values on Table 18.

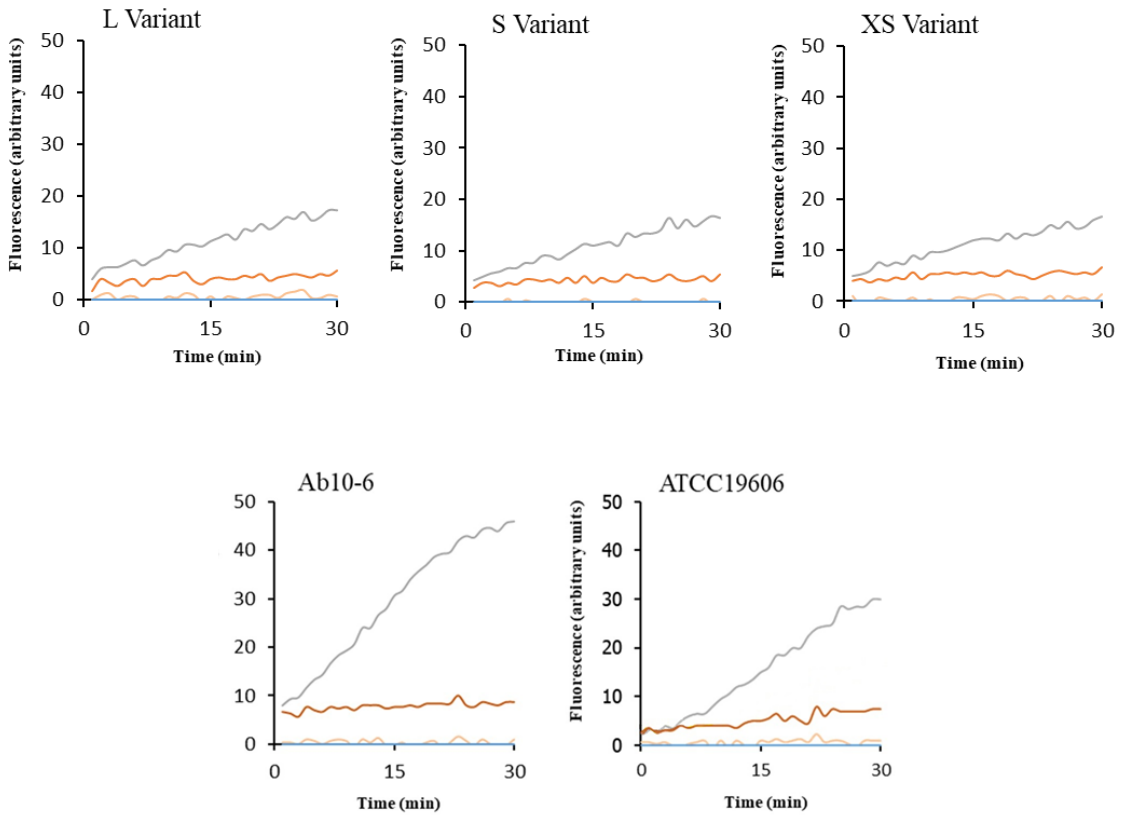

Figure 12. Effect of efflux inhibitor on EtBr accumulation in the absence of glucose. Equilibrium EtBr concentration used: 4 µg/mL for Ab10-6 and XS variant; and 2 µg/ml for S variant, L variant and ATCC19606. **TZ**, thioridazine (tested at 22.5 µM); **EtBr**, ethidium bromide; **Cell**, isolate + PBS; **PBS**, phosphate-buffered saline.

Table 18. Relative final fluorescence (RFF) values obtained from the efflux inhibitor TZ and their standard deviation.

Strain/ Variant	TZ inhibitor assay free of glucose RFF ± standard deviation
ATCC19606	**3.33** ± 0.47
Ab10-6	**4.02** ± 0.29
L Variant	**2.32** ± 0.26
S Variant	**1.86** ± 0.2
XS Variant	**1.82** ± 0.32

RFF, relative final fluorescence values above 1 (bold) were considered significant. TZ, thioridazine.

The RFF values were calculated from assays performed in duplicate and using the formula described in sub-topic 2.2.3.6.3. of the Material and Methods section. The RFF reflects the ability of an efflux inhibitor to potentiate EtBr retention within the cell, and the greater the difference between the RF value in the presence of the inhibitor compared to the RF of the isolate in the presence of the EtBr substrate alone, the greater the inhibitory effect on the efflux systems. Thus, all variants and the parental strain demonstrated active efflux systems. The L variant proved to be the variant with the highest RFF values among the isolated subpopulations, indicating that, contrary to what was suggested by the results obtained in the checkerboard assay and in the time-kill assay, this variant when tested by the direct detection method presents active efflux systems. Regarding the parental strain, the RFF values were higher when compared to the results for ATCC19606, meaning that Ab10-6 strain has greater efflux activity than the reference strain.

3.9.3. Detection of ethidium bromide efflux

Afterwards, the study was carried out by measuring the amount of EtBr that is effluxed by the cells. For this, the cells were incubated under conditions that promoted the accumulation of EtBr inside them and its fluorescence was subsequently measured when cells were submitted to an efflux favourable environment resulting in the determination of the relative fluorescence value that serve as an indicator of efflux activity. The results can be analysed in Figure 13.

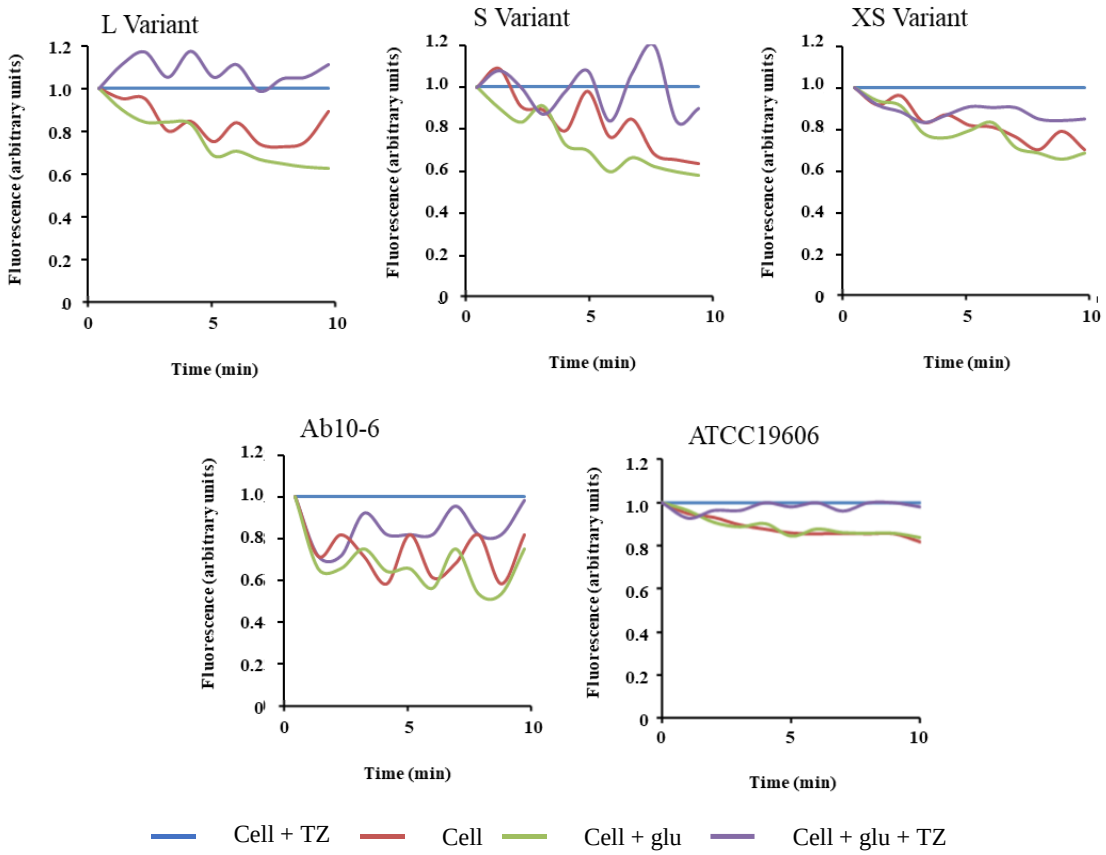

Figure 13. EtBr efflux assay in the presence of the inhibitor of efflux systems. **Cell**, isolate; **TZ**, thioridazine; **glu**, glucose.

By analysing the graphs presented in Figure 13, it is shown all the variants and the parental strain have high efflux activity that is inhibited in the presence of thioridazine. Among them, efflux activity is most pronounced in the L variant, followed by the S variant and ultimately the XS variant. The extensive overexpression of efflux pumps is confirmed in the assay performed in the presence of glucose which has a positive influence on efflux activity.

3.10. Evaluation of expression levels of genes encoding for efflux pumps in response to colistin exposure by RT-qPCR

Next, we proposed to study the relative expression levels of selected genes encoding efflux pumps in *A. baumannii*, with the aim of identifying the existence of efflux pumps overexpression in response to colistin exposure. First, to assess the presence of the efflux pumps chosen (Table 2, section 2.1.2. of Material and Methods), and to analyse the amplification efficiency that guarantees reliable RT-qPCR tests, the genes were amplified

by PCR for all isolates including reference strain ATCC19606. Once the presence of all genes encoding for efflux pumps were confirmed, the relative expression was evaluated.

The relative expression levels of the chosen genes encoding efflux pumps in *A. baumannii* were obtained by comparing the relative amount of mRNA in the presence and absence of colistin from the same isolate. The results of the quantification of the expression levels of each gene in the presence of colistin are described in Table 19.

Table 19. Quantification by RT-qPCR of expression levels of genes encoding efflux pumps in *A. baumannii* strains and variants, in the presence of colistin at ¼ of the MIC.

Gene	Relative expression level (mean ± standard deviation)				
	ATCC19606	Ab10-6	L Variant	S Variant	XS Variant
adeB	0.51 ± 0.22	**10.56 ± 0.00**	-6.9 ± 0.99	-1.5 ± 0.00	-1.9 ± 0.3
adeG	0.09 ± 0.02	**2.2 ± 0.7**	**2.0 ± 0.85**	**4.7 ± 0.3**	1.0 ± 0.1
adeJ	0.32 ± 0.09	1.20 ± 0.13	-0.5 ± 2.26	-0.2 ± 0.1	-1.5 ± 0.2
craA	1.19 ± 0.04	0.09 ± 0.03	**7.7 ± 0.57**	**5.4 ± 0.1**	1.1 ± 0.05
amvA	**37.11 ± 5.11**	1.4 ± 0.6	-0.6 ± 0.35	1.4 ± 0.05	0.9 ± 0.15
abeM	0.50 ± 0.38	0.5 ± 0.2	**2.0 ± 0.99**	**3.1 ± 0.00**	-0.3 ± 0.05
abeS	0.35 ± 0.00	-1.7 ± 0.15	1.5 ± 0.28	**4.2 ± 0.1**	-0.2 ± 0.45

A relative expression level of 1 indicates that the gene expression level is equal to that of the strain being compared. Over-expression is considered to exist for values equal to or greater than 2. Each assay was performed in triplicate.

Regarding efflux pump-mediated resistance in Gram-negative bacteria, the Resistance Nodulation and cell Division (RND) family is considered to represent the most clinically relevant pumps that confer resistance to multiple antimicrobial compounds. This family of efflux pumps consists of an inner membrane protein connected by a major fusion protein to an outer membrane factor, allowing bacterial cells to cross the inner and outer membranes and conferring the ability to extrude a wide range of substrates that are often

not directly related in structure to those of the efflux pump (Coyne, Courvalin and Périchon, 2011).

In this work, the relative expression of the multidrug transporter AdeB, encoded by the *adeABC* operon was evaluated. The *adeABC* operon was the first RND system characterized in *A. baumannii* (Coyne, Courvalin and Périchon, 2011), and is associated with resistance to β-lactams, fluoroquinolones, aminoglycoside, tetracyclines, macrolides, chloramphenicol, tigecycline, trimethoprim and carbapenems (Magnet, Courvalin and Lambert, 2001; Héritier *et al.*, 2005; Damier-Piolle *et al.*, 2008; Coyne, Courvalin and Périchon, 2011; Rodrigues, 2019). Its overexpression is also related to the contribution to colistin heteroresistance in clinical isolates (Park and Ko, 2015; Machado *et al.*, 2018; Chen *et al.*, 2020; Gothe, 2020). In this study the parental strain was found to overexpress the *abeB* gene in the presence of colistin, whereas its variants have a downregulated gene expression, indicating that different response in efflux pumps expression can be found in a clinical isolate with heteroresistance to colistin.

The *adeIJK* operon was the second RND efflux system described in *A. baumannii*. It contributes to resistance to aztreonam, fluoroquinolones, tetracyclines, tigecycline, lincosamides, rifampicin, chloramphenicol, co-trimoxazole, novobiocin, fusidic acid and contributes to intrinsic resistance to β-lactams (Damier-Piolle *et al.*, 2008; Coyne, Courvalin and Périchon, 2011). In this study, no overexpression of the *adeJ* gene was detected in any of the variants or the parental strain when exposed to colistin. However, overexpression of the *adeJ* gene when exposed to colistin has been described in *A. baumannii* clinical isolates presenting heteroresistance to colistin (Ni *et al.*, 2016; Machado *et al.*, 2018; Chen *et al.*, 2020; Gothe, 2020).

The third RND system present in *A. baumannii* corresponds to the AdeFGH efflux pump. When overexpressed, this efflux pump, encoded by the *adeFGH* operon, is associated with an MDR profile (Coyne, Courvalin and Périchon, 2011). It confers resistance to fluoroquinolones, chloramphenicol, trimethoprim, clindamycin, tetracyclines, tigecycline, and sulfamethoxazole (Coyne *et al.*, 2010). Overexpression of the *abeG* gene, one of the structural genes of the *adeFGH* operon, was detected in *A. baumannii* clinical isolates when exposed to carbapenem and in clinical isolates with heteroresistance to colistin (Machado *et al.*, 2018; Rodrigues, 2019; Chen *et al.*, 2020). Analysing the relative

expression of this gene in the different variants, a disparity in response to colistin exposure was observed. The S variant has an overexpression level of 4.7 and the L variant presents an overexpression level of 2, whereas the XS variant shows no overexpression. One mechanism described by which overexpression of the *adeFGH* operon may occur corresponds to the presence of mutations in its putative regulator AdeL (Coyne, Courvalin and Périchon, 2011). It would be interesting in future studies to analyse if the same occurs in these clinical isolates. These results demonstrate that even if the parental strain presents the *adeG* gene overexpressed, it may differ when analysing the different subpopulations that constitute it.

Unlike RND efflux systems which can extrude a wide range of substrates, *A. baumannii* has single-component efflux systems that provide resistance to a small number of compounds. These efflux pumps only cross the inner cell membrane, allowing extrusion from inside the cell into the periplasm (Coyne, Courvalin and Périchon, 2011).

In *A. baumannii*, the efflux of antimicrobial compounds in single-component efflux systems is mainly due to the activity of transporters belonging to the major facilitator superfamily (MFS), and is therefore, associated with multidrug resistance phenotypes (Vila, Martí and Sánchez-Céspedes, 2007).

In this study, the relative expression of two efflux pumps belonging to this family were analysed. The AmvA efflux pump, intrinsic in *A. baumannii*, responsible for the efflux of dyes, detergents, disinfectants and erythromycin (Rajamohan, Srinivasan and Gebreyes, 2010; Coyne, Courvalin and Périchon, 2011), and when overexpressed is apparently related to resistance to various antibiotics, such as aminoglycosides, fluoroquinolones, cephalosporins and carbapenems (Rajamohan, Srinivasan and Gebreyes, 2010; Ling, Zhang and Li, 2016). In this work, only the reference strain ATCC19606 showed an overexpression of the *amvA* gene after exposure to colistin.

The second efflux pump belonging to the MFS family for which relative expression levels were analysed was the CraA efflux pump. In *A. baumannii* this efflux pump is associated with intrinsic resistance to the antibiotic chloramphenicol (Roca *et al.*, 2009), and its overexpression was found in clinical isolates when exposed to colistin (Machado *et al.*, 2018). In this study, the L variant and S variant displayed high overexpression of this

gene, while the XS variant, parental strain, and reference strain ATCC19606 did not exhibit overexpression.

The multidrug and toxic compound extrusion (MATE) family is also part of the efflux systems that are associated with drug resistance in *A. baumannii* (Su *et al.*, 2005; Coyne, Courvalin and Périchon, 2011). The AbeM efflux pump is a member of the MATE family and is associated with the extrusion of aminoglycosides, fluoroquinolones, chloramphenicol, trimethoprim, ethidium bromide, and dyes (Su *et al.*, 2005). Its overexpression was found in clinical isolates of *A. baumannii* when exposed to imipenem and colistin (Machado *et al.*, 2018; Rodrigues, 2019). In this study, the *abeM* gene was overexpressed in the S and L variants, and at basal levels in the XS variant, parental strain, and reference strain.

The last efflux pump for which relative expression levels were analysed was the AbeS efflux pump. This efflux pump belongs to the small multidrug resistance (SMR) family and is associated with resistance to chloramphenicol, fluoroquinolones, erythromycin, novobiocin, as well as resistance to dyes and detergents (Coyne, Courvalin and Périchon, 2011). Overexpression of this gene was observed in the S variant and basal levels in the other variants, parental strain, and reference strain. The overexpression of the *abeS* gene has been reported in clinical isolates when exposed to imipenem and colistin (Machado *et al.*, 2018; Rodrigues, 2019), and in this study on a subpopulation of an *A. baumannii* clinical isolate with heteroresistance to colistin.

4. Final considerations

Current treatment of *A. baumannii* infections is problematic due to its widespread MDR phenotype, the lack of novel drugs for the treatment of these serious infections, and the existence of heteroresistance that may be a preliminary stage that leads to the proliferation of resistant subpopulations upon exposure to colistin (Li *et al.*, 2006; Machado *et al.*, 2018). Colistin resistance has gained global attention and poses a new threat to public health, despite their relatively recent reintroduction in clinical practice, reports on colistin resistant isolates are on the rise (Falagas, Rafailidis and Matthaiou, 2010; Olaitan, Morand and Rolain, 2014; Huang *et al.*, 2017; Machado *et al.*, 2018; Rodrigues, 2019).

In this study we proposed to characterise the possible mechanisms underlying the appearance of heteroresistance phenotype in a clinical isolate of carbapenemase-producing MDR *A. baumannii* with simultaneous resistance to colistin. For this purpose, three subpopulations were isolated based on morphological differences demonstrated in SuperPolymyxin medium, and an antimicrobial susceptibility testing was performed where variants presented a diverse resistance profile. Also, colistin MIC, even though over the clinical breakpoint, differed among the three variants with the L variant presenting the lowest value with 16 μg/mL, 16-fold lower than the XS variant and 8-fold lower than the S variant. Variant L also showed the lowest growth rate and when tested in the presence of colistin and the efflux inhibitor TZ was able to overcome the bactericidal effect observed for variants S, XS, parental strain Ab10-6 and reference strain ATCC19606. When the indirect effect of efflux pump activity on colistin resistance was assessed, only variant S showed reduced levels of resistance in the presence of the efflux inhibitor, indicating that there might be more than one mechanism involved in colistin heteroresistance phenotype in variants L and XS. However, when evaluated by the direct method of efflux activity detection, all variants showed increased efflux activity especially L variant. Also, the overexpression of the efflux pumps was detected for the L variant and for the S variant. The XS variant did not show overexpression for the analysed efflux pump genes. Demonstrating that the mutations confer a stable phenotype of resistance to the XS variant, while in the L and S variants there appear to be several mechanisms involved in colistin resistance. All variants as well as the parental strain show the same chromosomal mutations in the genes associated with colistin resistance, with a

double mutation in the *pmrB* gene (L271R and N440H), and a single mutation in the *lpxC* and *lpxD* genes (N287D and E117K, respectively), with no changes observed for the *pmrA* and *lpxA* gene. None of these mutations are, to our knowledge, described in these genes.

Evidence that efflux activity contributes to a high level of resistance to colistin in the S variant and parental strain Ab10-6, inferred by reduced MIC of colistin in the presence of subinhibitory concentrations of thioridazine, despite the presence of resistance-conferring mutations in genes associated with colistin resistance, contradicts the dogma that the activity of efflux only confers resistance in strains without mutations associated with resistance to a particular antimicrobial compound (Li, Livermore and Nikaido, 1994). This dogma has been challenged in several studies involving different microorganisms such as *Salmonella enterica* serovar Typhimurium (Chen *et al.*, 2007), *S. aureus* (Costa *et al.*, 2011), *Mycobacterium tuberculosis* (Machado *et al.*, 2017), *Mycobacterium avium* (Machado *et al.*, 2015), *A. baumannii* (Rodrigues, 2019; Chen *et al.*, 2020; Gothe, 2020) and again in *A. baumannii* in this study.

An important characteristic of the heteroresistance phenotype is its stability. When a highly resistant subpopulations reverts, in the absence of antibiotic pressure, to the heterogeneous resistance phenotype exhibited by the original population, it is defined as an unstable heteroresistant phenotype (Sutherland and Rolinson, 1964; Lencastre, Figueiredo and Tomasz, 1993; Plipat *et al.*, 2005; Pournaras *et al.*, 2010; El-Halfawy and Valvano, 2015; Anderson *et al.*, 2018; Andersson, Nicoloff and Hjort, 2019; Nicoloff *et al.*, 2019; Pereira *et al.*, 2021). Whereas others retain their high-level resistance (Søgaard, 1985; Plipat *et al.*, 2005; El-Halfawy and Valvano, 2013, 2015; Anderson *et al.*, 2018; Machado *et al.*, 2018; Nicoloff *et al.*, 2019). In this study, the heteroresistance phenotype of these strain variants was maintained even when grown without antibiotic pressure. In all strain variants mutations were detected in genes associated with colistin resistance in *A. baumannii*, further studies should be carried out to understand whether these mutations are partially responsible for the resistance phenotype using molecular genetics approaches. Since a large morphological difference was observed between the clinical strain variants, analysis of cell wall morphology and composition by transmission

electron microscopy and GC/MS, and population analysis profiling should be performed to better determine the mechanisms underlying colistin heteroresistance in *A. baumannii*.

Furthermore, an important virulence mechanism in nosocomial infections of *A. baumannii* is its high capacity to form biofilms, easily prevailing in adverse environments and enabling the development of high resistance to antimicrobials (Peleg, Seifert and Paterson, 2008). Chemical communication can also mediate heteroresistance between bacterial species (El-Halfawy and Valvano, 2013), therefore, the ability of the different subpopulations to form biofilms is also an important point to be developed in future studies to better describe the multitude of features that allows *A. baumannii* to continue to be the opportunistic pathogen with the highest level of urgency for the development and discovery of new antimicrobial compounds.

5. References

Adams, M.D. *et al.* (2009). Resistance to colistin in *Acinetobacter baumannii* associated with mutations in the PmrAB two-component system. *Antimicrob. Agents and Chemother*. 53(9): 3628–3634. doi: 10.1128/AAC.00284-09

Alexander, H.E. and Leidy, G. (1947). Mode of action of streptomycin on type B *H. Influenzae*. *J. Exp. Med*. 85(4): 329–338.

Anderson, S.E. *et al.* (2018). Aminoglycoside heteroresistance in *Acinetobacter baumannii* AB5075. *mSphere*. 3(4): e00271-18. doi: 10.1128/mSphere.00271-18

Andersson, D.I., Nicoloff, H. and Hjort, K. (2019). Mechanisms and clinical relevance of bacterial heteroresistance. *Nat. Rev. Microbiol.* 17(8): 479–496. doi: 10.1038/s41579-019-0218-1.

Antunes, L.C.S., Visca, P. and Towner, K.J. (2014). *Acinetobacter baumannii*: evolution of a global pathogen. *Pathog. Dis.* 71(3): 292–301. doi: 10.1111/2049-632X.12125.

Arroyo, L.A. *et al.* (2011). The *pmrCAB* operon mediates polymyxin resistance in *Acinetobacter baumannii* ATCC 17978 and clinical isolates through phosphoethanolamine modification of lipid A. *Antimicrob. Agents Chemother*. 55(8): 3743–3751. doi: 10.1128/AAC.00256-11.

Asif, M., Alvi, I.A. and Rehman, S.U. (2018). Insight into *Acinetobacter baumannii*: pathogenesis, global resistance, mechanisms of resistance, treatment options, and alternative modalities. *Infect. Drug Resist.* 11: 1249–1260. doi: 10.2147/IDR.S166750.

Beceiro, A. *et al.* (2011). Phosphoethanolamine modification of lipid A in colistin-resistant variants of *Acinetobacter baumannii* mediated by the *pmrAB* two-component regulatory system. *Antimicrob. Agents Chemother.* 55(7): 3370–3379. doi: 10.1128/AAC.00079-11

Bergogne-Bérézin, E., Friedman, H. and Bendinelli, M. (eds) (2008). *Acinetobacter Biology and Pathogenesis*. New York, NY: Springer US (Infectious Agents and Pathogenesis). doi: 10.1007/978-0-387-77944-7.

Brooks, G. *et al.* (2012). Jawetz Melnick & Adelbergs Medical Microbiology 26th ed. Blacklick: McGraw-Hill Publishing.

Bustin, S.A. (2000). Absolute quantification of mRNA using real-time reverse transcription polymerase chain reaction assays. *J. Mol. Endocrinol.* 25(2): 169–193.

Bustin, S.A. *et al.* (2009). The MIQE Guidelines: minimum information for publication of quantitative real-time PCR experiments. *Clin. Chem.* 55(4): 611–622. doi: 10.1373/clinchem.2008.112797.

Chen, L. *et al.* (2020). Deciphering colistin heteroresistance in *Acinetobacter baumannii* clinical isolates from Wenzhou, China. *J. Antibiot.* 73(7): 463–470. doi: 10.1038/s41429-020-0289-2.

Chen, S. *et al.* (2007). Contribution of target gene mutations and efflux to decreased susceptibility of *Salmonella enterica* serovar Typhimurium to fluoroquinolones and other antimicrobials. *Antimicrob. Agents Chemother.* 51(2): 535–542. doi: 10.1128/AAC.00600-06

Chusri, S. *et al.* (2014). Clinical outcomes of hospital-acquired infection with *Acinetobacter nosocomialis* and *Acinetobacter pittii*. *Antimicrob. Agents Chemother.* 58(7): 4172–4179. doi: 10.1128/AAC.02992-14.

Clinical and Laboratory Standards Institute (CLSI) (2020). Performance standards for antimicrobial susceptibility testing. 30th ed. CLSI supplement M100. Clinical and Laboratory Standards Institute, 950 West Valley Road, Suite 2500, Wayne, Pennsylvania 19087 USA.

Clinical and Laboratory Standards Institute (CLSI) (2018). Performance standards for antimicrobial susceptibility testing. 28th ed. CLSI seventeenth informational supplement. M100-S17. Clinical and Laboratory Standards Institute, 950 West Valley Road, Suite 2500, Wayne, Pennsylvania 19087 USA.

Colman, R.E. *et al.* (2015). Detection of low-level mixed-population drug resistance in *Mycobacterium tuberculosis* using high fidelity amplicon sequencing. PLoS ONE 10(5): e0126626. doi: 10.1371/journal.pone.0126626.

Costa, S.S. *et al.* (2011). Exploring the contribution of efflux on the resistance to fluoroquinolones in clinical isolates of *Staphylococcus aureus. BMC Microbiol.* 11(1): 1–12.

Coyne, S. *et al.* (2010). Overexpression of resistance-nodulation-cell division pump AdeFGH confers multidrug resistance in *Acinetobacter baumannii*. *Antimicrob. Agents Chemother*. 54(10): 4389–4393. 10.1128/AAC.00155-10.

Coyne, S., Courvalin, P. and Périchon, B. (2011). Efflux-mediated antibiotic resistance in *Acinetobacter* spp. *Antimicrob. Agents Chemother.* 55(3): 947–953. doi: 10.1128/AAC.01388-10.

Damier-Piolle, L. *et al.* (2008). AdeIJK, a resistance-nodulation-cell division pump effluxing multiple antibiotics in *Acinetobacter baumannii*. *Antimicrob. Agents Chemother.* 52(2): 557–562. doi: 10.1128/AAC.00732-07.

Davis, K.A. *et al.* (2005). Multidrug-resistant *Acinetobacter* extremity infections in soldiers. *Emerg. Infect. Dis.* 11(8): 1218–1224. doi: 10.3201/1108.050103.

DeMarco, C.E. *et al.* (2007). Efflux-related resistance to norfloxacin, dyes, and biocides in bloodstream isolates of *Staphylococcus aureus*. *Antimicrob. Agents Chemother.* 51(9): 3235–3239. doi: 10.1128/AAC.00430-07.

Demirdal, T., Sari, U.S. and Nemli, S.A. (2016). Is inhaled colistin beneficial in ventilator associated pneumonia or nosocomial pneumonia caused by *Acinetobacter baumannii*? *Ann. Clin. Microbiol. Antimicrob.* 15(1): 11. doi: 10.1186/s12941-016-0123-7.

Deris, Z.Z. *et al.* (2014). A secondary mode of action of polymyxins against Gram-negative bacteria involves the inhibition of NADH-quinone oxidoreductase activity. *J. Antibiot.* 67(2): 147–151. doi: 10.1038/ja.2013.111.

Deveson Lucas, D. *et al.* (2018). Emergence of high-level colistin resistance in an *Acinetobacter baumannii* clinical isolate mediated by inactivation of the global regulator H-NS. *Antimicrob. Agents Chemother.* 62(7): e02442-17. doi: 10.1128/AAC.02442-17.

Dijkshoorn, L., Nemec, A. and Seifert, H. (2007). An increasing threat in hospitals: multidrug-resistant *Acinetobacter baumannii*. *Nat. Rev. Microbiol.* 5(12): 939–951. doi: 10.1038/nrmicro1789.

Dijkshoorn, L. and van der Toorn, J. (1992). *Acinetobacter* species: which do we mean? *Clin. Microbiol. Infect.* 15(4): 748–749. doi: 10.1093/clind/15.4.748.

Division of Laboratory Systems (DLS) (2020). Colonial characteristics, biochemicals and Gram-negative organism ID. https://www.cdc.gov/labtraining/docs/job_aids/biochemicals_and_gram-negative_organism_id/Colonial_Characteristics_Branded_508.pdf. Accessed 24 September 2022.

Durand-Réville, T.F. *et al.* (2017). ETX2514 is a broad-spectrum β-lactamase inhibitor for the treatment of drug-resistant Gram-negative bacteria including *Acinetobacter baumannii*. *Nat. Microbiol.* 2(9): 17104. doi: 10.1038/nmicrobiol.2017.104.

El-Halfawy, O.M. and Valvano, M.A. (2013). Chemical communication of antibiotic resistance by a highly resistant subpopulation of bacterial cells. *PLoS ONE* 8(7): e68874. doi: 10.1371/journal.pone.0068874.

El-Halfawy, O.M. and Valvano, M.A. (2015). Antimicrobial heteroresistance: an emerging field in need of clarity. *Clin. Microbiol. Rev.* 28(1): 191–207. doi: 10.1128/CMR.00058-14.

European Committee on Antimicrobial Susceptibility Testing (EUCAST) (2020). Breakpoint tables for interpretation of MICs and zone diameters. Version 10.0. https://www.eucast.org/ast_of_bacteria/previous_versions_of_documents.

European Committee on Antimicrobial Susceptibility Testing (EUCAST) (2017). Breakpoint tables for interpretation of MICs and zone diameters. Version 7.1. https://www.eucast.org/ast_of_bacteria/previous_versions_of_documents.

Euzéby, J.P. (1997). List of bacterial names with standing in nomenclature: a folder available on the internet. *Int. J. Syst. Evol. Microbiol.* 47(2): 590–592. doi: 10.1099/00207713-47-2-590.

Falagas, M.E. *et al.* (2007). Community-acquired *Acinetobacter* infections. *Eur. J. Clin. Microbiol. Infect. Dis.* 26(12): 857–868. doi: 10.1007/s10096-007-0365-6.

Falagas, M.E., Rafailidis, P.I. and Matthaiou, D.K. (2010). Resistance to polymyxins: mechanisms, frequency and treatment options. *Drug Resist. Updat.* 13(4–5): 132–138. doi: 10.1016/j.drup.2010.05.002.

Fishbain, J. and Peleg, A.Y. (2010). Treatment of *Acinetobacter* infections. *Clin. Infect. Dis.* 51(1): 79–84. doi: 10.1086/653120.

Gothe, S. (2020). Heterorresistência à colistina em estirpes de *Acinetobacter baumannii* produtoras de carbapenemases: o papel das bombas de efluxo. Graduation project. Universidade Lusófona de Humanidade e Tecnologias, Lisboa, Portugal.

Gröblacher, B., Kunert, O. and Bucar, F. (2012). Compounds of *Alpinia katsumadai* as potential efflux inhibitors in *Mycobacterium smegmatis*. *Bioorg. Med. Chem.* 20(8): 2701–2706. doi: 10.1016/j.bmc.2012.02.039.

Héritier, C. *et al.* (2005). Characterization of the naturally occurring oxacillinase of *Acinetobacter baumannii*. *Antimicrob. Agents Chemother.* 49(10): 4174–4179. doi: 10.1128/AAC.49.10.4174-4179.2005.

Hjort, K., Nicoloff, H., and Andersson, D.I. (2016). Unstable tandem gene amplification generates heteroresistance (variation in resistance within a population) to colistin in *Salmonella enterica*. *Mol. Microbiol.* 102(2): 274–289. doi: org/10.1111/mmi.13459.

Hong, Y.K., Kim, H., and Ko, K.S. (2020). Two types of colistin heteroresistance in *Acinetobacter baumannii* isolates. *Emerg. Microbes Infect.* 9(1): 2114-2123. doi: 10.1080/22221751.2020.1821584.

Huang, X. *et al.* (2017). High prevalence of colistin resistance and *mcr*-1 gene in *Escherichia coli* isolated from food animals in China. *Front. Microbiol*. 8: 562. doi: 10.3389/fmicb.2017.00562.

Hudzicki, J. (2009). Kirby-Bauer disk diffusion susceptibility test protocol. American Society for Microbiology. 15: 55–63. Available at https://asm.org/getattachment/2594ce26-bd44-47f6-8287-0657aa9185ad/Kirby-Bauer-Disk-DiffusionSusceptibility-Test-Protocol-pdf.pdf.

Jones, R.N. *et al.* (2007). Multicenter studies of tigecycline disk diffusion susceptibility results for *Acinetobacter* spp. *J. Clin. Microbiol*. 45(1): 227–230. doi: 10.1128/JCM.01588-06.

Kalil, A.C., *et al.* (2016). Management of adults with hospital-acquired and ventilator-associated pneumonia: 2016 clinical practice guidelines by the Infectious Diseases Society of America and the American Thoracic Society. *Clin. Infect. Dis.* 63(5): e61–e111. doi: 10.1093/cid/ciw353.

Karageorgopoulos, D.E. and Falagas, M.E. (2008). Current control and treatment of multidrug-resistant *Acinetobacter baumannii* infections. *Lancet Infect Dis.* 8(12): 751–762. doi: 10.1016/S1473-3099(08)70279-2.

Kim, Y., *et al.* (2014). In vivo emergence of colistin resistance in *Acinetobacter baumannii* clinical isolates of sequence type 357 during colistin treatment. *Diagn. Microbiol. Infect. Dis.* 79(3): 362–366. doi: 10.1016/j.diagmicrobio.2014.03.027.

Kyriakidis, I., *et al.* (2021). *Acinetobacter baumannii* antibiotic resistance mechanisms. *Pathogens*. 10(3): 373. doi: 10.3390/pathogens10030373.

Łapińska, U., *et al.* (2022). Fast bacterial growth reduces antibiotic accumulation and efficacy. *eLife*. 11: e74062. doi: 10.7554/eLife.74062.

Lee, H.-Y., *et al.* (2011). Imipenem heteroresistance induced by imipenem in multidrug-resistant *Acinetobacter baumannii*: mechanism and clinical implications. *Int. J. Antimicrob. Agents*. 37(4): 302-308. doi: 10.1016/j.ijantimicag.2010.12.015.

Leggett, H.C., *et al.* (2017). Growth rate, transmission mode and virulence in human pathogens. *Phil. Trans. R. Soc. B.* 372: 20160094. doi: 10.1098/rstb.2016.0094.

Lencastre, H., Figueiredo, A.M.S. and Tomasz, A. (1993). Genetic control of population structure in heterogeneous strains of methicillin resistant *Staphylococcus aureus*. *Eur. J. Clin. Microbiol. Infect. Dis.* 12(S1): S13–S18. doi: 10.1007/BF02389872.

Levine, M. (1943). The effect of concentration of dyes on differentiation of enteric bacteria on eosin-methylene-blue agar. *J. Bacteriol.* 45(5): 471–475. doi: 10.1128/jb.45.5.471-475.1943.

Li, J., *et al.* (2005). Evaluation of colistin as an agent against multi-resistant Gram-negative bacteria. *Int. J. Antimicrob. Agents.* 25(1): 11–25. doi: 10.1016/j.ijantimicag.2004.10.001.

Li, J. *et al.,* (2006). Heteroresistance to colistin in multidrug-resistant *Acinetobacter baumannii*. *Antimicrob. Agents Chemother.* 50(9): 2946–2950. doi: 10.1128/AAC.00103-06.

Li, X.-Z., Livermore, D.M. and Nikaido, H. (1994). Role of efflux pump(s) in intrinsic resistance of *Pseudomonas aeruginosa*: resistance to tetracycline, chloramphenicol, and norfloxacin. *Antimicrob. Agents Chemother.* 38(8): 1732–1741. doi: 10.1128/AAC.38.8.1732.

Liang, W. *et al.,* (2011). Activities of colistin- and minocycline-based combinations against extensive drug resistant *Acinetobacter baumannii* isolates from intensive care unit patients. *BMC Infect. Dis.* 11(1): 109. doi: 10.1186/1471-2334-11-109.

Ling, B.D., Zhang L. & Li, X. Z. (2016). Antimicrobial resistance and drug efflux pumps in *Acinetobacter*. *In* Efflux-Mediated Antimicrobial Resistance in Bacteria. Mechanisms, Regulation and Clinical Implications. Li, X., Elkins, C. A. & Zgurskaya, H. I. Eds.; Adis, Cham – Springer International Publishing, Switzerland; pp.329-358.

Liu, J. *et al.* (2021). Comparative efficacy and safety of combination therapy with high-dose sulbactam or colistin with additional antibacterial agents for multiple drug-resistant and extensively drug-resistant *Acinetobacter baumannii* infections: a systematic review and network meta-analysis. *J. Glob. Antimicrob. Resist.* 24: 136–147. doi: 10.1016/j.jgar.2020.08.021.

Livak, K.J. and Schmittgen, T.D. (2001). Analysis of relative gene expression data using real-time quantitative PCR and the 2−ΔΔCT method. *Methods*. 25(4): 402–408. doi: 10.1006/meth.2001.1262.

López-Rojas, R. *et al.* (2011). *Acinetobacter baumannii* resistant to colistin alters its antibiotic resistance profile: a case report from Spain. *J. Infect. Dis.* 204(7): 1147–1148. doi: 10.1093/infdis/jir476.

Machado, D. *et al.* (2015). Boosting effect of 2-phenylquinoline efflux inhibitors in combination with macrolides against *Mycobacterium smegmatis* and *Mycobacterium avium*. *ACS Infect. Dis.* 1(12): 593–603. 10.1021/acsinfecdis.5b00052.

Machado, D. *et al.* (2017). Interplay between mutations and efflux in drug resistant clinical isolates of *Mycobacterium tuberculosis*. *Front. Microbiol.* 8: 711. doi: 10.3389/fmicb.2017.00711.

Machado, D. *et al.* (2018). Contribution of efflux to colistin heteroresistance in a multidrug resistant *Acinetobacter baumannii* clinical isolate. *J. Med. Microbiol.* 67(6): 740–749. doi: 10.1099/jmm.0.000741.

Machado, L. *et al.* (2011). Biological activity of twenty-three hydantoin derivatives on intrinsic efflux pump system of Salmonella enterica serovar Enteritidis NCTC 13349. *In vivo*. 25: 769-772.

Magnet, S., Courvalin, P. and Lambert, T. (2001). Resistance-nodulation-cell division-type efflux pump involved in aminoglycoside resistance in *Acinetobacter baumannii* strain BM4454. *Antimicrob. Agents Chemother.* 45(12): 3375–3380. doi:10.1128/AAC.45.12.3375-3380.2001

Manchanda, V., Sinha, S. and Singh, N. (2010). Multidrug resistant *Acinetobacter*. *J. Glob. Infect. Dis.* 2(3): 291–304. doi: 10.4103/0974-777X.68538.

Manjunath, A. *et al.* (2021). Bacterial heteroresistance: an evolving novel way to combat antibiotics. *Biologia*. 76(10): 3029–3041. doi: 10.1007/s11756-021-00820-y.

Mascellino, M.T. *et al.* (2017). Antibiotic susceptibility, heteroresistance, and updated treatment strategies in *Helicobacter pylori* infection. *Drug Des. Devel. Ther*. 11: 2209–2220. doi: 10.2147/DDDT.S136240.

McLeod, S.M. *et al.* (2020). *In vitro* activity of sulbactam-durlobactam against *Acinetobacter baumannii-calcoaceticus* complex isolates collected globally in 2016 and 2017. *Antimicrob. Agents Chemother*. 64(4): e02534-19. doi: 10.1128/AAC.02534-19.

Mendes, R.E. *et al.* (2008). Increased antimicrobial susceptibility profiles among polymyxin-resistant *Acinetobacter baumannii* clinical isolates. *Clin. Infect. Dis.* 46(8): 1324–1326. doi: 10.1086/533476.

Moffatt, J.H. *et al.* (2010). Colistin resistance in *Acinetobacter baumannii* is mediated by complete loss of lipopolysaccharide production. *Antimicrob. Agents Chemother*. 54(12): 4971–4977. doi:10.1128/AAC.00834-10.

Moffatt, J.H. *et al.* (2011). Insertion sequence IS*Aba11* is involved in colistin resistance and loss of lipopolysaccharide in *Acinetobacter baumannii*. *Antimicrob. Agents Chemother*. 55(6): 3022–3024. doi: 10.1128/AAC.01732-10.

Moody, J.A. (1992). Synergism testing: broth microdilution checkerboard and broth macrodilution methods. Washington DC. American Society for Microbiology.

Morrison, T.B., Weis, J.J., and Wittwer, C.T. (1998). Quantification of low-copy transcripts by continuous SYBR Green I monitoring during amplification. *Biotechniques*. 24(6): 954-962.

Ni, W. *et al.* (2016). Effects of efflux pump inhibitors on colistin resistance in multidrug-resistant Gram-negative bacteria. *Antimicrob. Agents Chemother*. 60(5): 3215–3218. 10.1128/AAC.00248-16.

Nicoloff, H. *et al.* (2019). The high prevalence of antibiotic heteroresistance in pathogenic bacteria is mainly caused by gene amplification. *Nat. Microbiol.* 4(3): 504–514. doi: 10.1038/s41564-018-0342-0.

Nolan, T., Hands, R.E. and Bustin, S.A. (2006). Quantification of mRNA using real-time RT-PCR. *Nat Protoc.* 1(3): 1559–1582. doi: 10.1038/nprot.2006.236.

Nordmann, P., Jayol, A. and Poirel, L. (2016). A universal culture medium for screening polymyxin-resistant Gram-negative isolates. *J. Clin. Microbiol.* 54(5): 1395–1399. doi.org/10.1128/JCM.00446-16.

Olaitan, A.O., Morand, S. and Rolain, J.-M. (2014). Mechanisms of polymyxin resistance: acquired and intrinsic resistance in bacteria. *Front. Microbiol.* 5: 643. doi: 10.3389/fmicb.2014.00643.

Owen, R.J. *et al.* (2007). In vitro pharmacodynamics of colistin against *Acinetobacter baumannii* clinical isolates. *J. Antimicrob. Chemother*. 59(3): 473–477. doi: 10.1093/jac/dkl512.

Paixão, L. *et al.* (2009). Fluorometric determination of ethidium bromide efflux kinetics in *Escherichia coli*. *J. Biol. Eng.* 3(1): 18. doi: 10.1186/1754-1611-3-18.

Park, Y.K. and Ko, K.S. (2015). Effect of carbonyl cyanide 3-chlorophenylhydrazone (CCCP) on killing *Acinetobacter baumannii* by colistin. *J. Microbiol.* 53(1): 53–59. doi: 10.1007/s12275-015-4498-5.

Parte, A.C. (2018). LPSN – List of prokaryotic names with standing in nomenclature (bacterio.net), 20 years on. *Int. J. Syst. Evol. Microbiol.* 68(6): 1825–1829. doi: 10.1099/ijsem.0.002786.

Peleg, A.Y., Seifert, H., and Paterson, D.L. (2008). *Acinetobacter baumannii*: Emergence of a successful pathogen. *Clin. Microbiol. Rev.* 21(3): 538–582. doi: 10.1128/CMR.00058-07.

Peng, C., Zong, Z. and Fan, H. (2012). *Acinetobacter baumannii* isolates associated with community-acquired pneumonia in West China. *Clin. Microbiol. Infect.* 18(12): E491–E493. doi: 10.1111/1469-0691.12017.

Pereira, C. *et al.* (2021). The highly dynamic nature of bacterial heteroresistance impairs its clinical detection. *Commun. Biol.* 4(1): 521. doi: 10.1038/s42003-021-02052-x.

Perez, F. *et al.* (2007). Global challenge of multidrug-resistant *Acinetobacter baumannii*. *J. Antimicrob. Chemother.* 51(10): 3471–3484. doi: 10.1128/AAC.01464-06.

Petrosillo, N., Ioannidou, E. and Falagas, M.E. (2008). Colistin monotherapy vs. combination therapy: evidence from microbiological, animal and clinical studies. *Clin. Microbiol. Infect.* 14(9): 816–827. doi: 10.1111/j.1469-0691.2008.02061.x.

Pfaffl, M.W. (2001). A new mathematical model for relative quantification in real-time RT-PCR. *Nucleic Acids Res.* 29(9): 45e. doi: 10.1093/nar/29.9.e45.

Pharmaceutics, W. (2005). Tygacil (tigecycline) for injection. Package insert. Philadelphia, PA: Wyeth Pharmaceuticals Inc.

Plipat, N. *et al.* (2005). Unstable vancomycin heteroresistance is common among clinical isolates of methicillin-resistant *Staphylococcus aureus*. *J. Clin. Microbiol.* 43(5): 2494–2496. doi: 10.1128/JCM.43.5.2494-2496.2005.

Poirel, L., Jayol, A. and Nordmann, P. (2017). Polymyxins: antibacterial activity, susceptibility testing, and resistance mechanisms encoded by plasmids or chromosomes. *Clin. Microbiol. Rev.* 30(2): 557–596. doi: 10.1128/CMR.00064-16.

Pournaras, S. *et al.* (2005). Heteroresistance to carbapenems in *Acinetobacter baumannii*. *J. Antimicrob. Chemother.* 55(6): 1055–1056. doi: 10.1093/jac/dki115.

Pournaras, S. *et al.* (2010). Characteristics of meropenem heteroresistance in *Klebsiella pneumoniae* carbapenemase (KPC)-producing clinical isolates of *K. pneumoniae*. *J. Clin. Microbiol.* 48(7): 2601–2604. doi: 10.1128/JCM.02134-09.

Rajamohan, G., Srinivasan, V.B. and Gebreyes, W.A. (2010). Molecular and functional characterization of a novel efflux pump, AmvA, mediating antimicrobial and disinfectant resistance in *Acinetobacter baumannii*. *J. Antimicrob. Chemother.* 65(9): 1919–1925. doi: 10.1093/jac/dkq195.

Ranjbar, R. *et al.* (2017). Enterobacterial repetitive intergenic consensus polymerase chain reaction (ERIC-PCR) genotyping of *Escherichia coli* strains isolated from different animal stool specimens. *Iran J. Pathol*. 12(1): 25–34. doi: 10.30699/ijp.2017.21506.

Richmond, G.E., Chua, K.L. and Piddock, L.J.V. (2013). Efflux in *Acinetobacter baumannii* can be determined by measuring accumulation of H33342 (bis-benzamide). *J. Antimicrob. Chemother*. 68(7): 1594–1600. doi: 10.1093/jac/dkt052.

Roca, I. *et al.* (2009). CraA, a major facilitator superfamily efflux pump associated with chloramphenicol resistance in *Acinetobacter baumannii*. *Antimicrob. Agents Chemother*. 53(9): 4013–4014. doi: 10.1128/AAC.00584-09.

Rodrigues, J. (2014). Testes de susceptibilidade aos antimicrobianos: laboratório online. https://www.fciencias.com/2014/01/23/testes-de-susceptibilidade-aos-antimicrobianos-laboratorio-online/. Accessed May 21, 2020.

Rodrigues, T. A. F. (2019). Caracterização dos mecanismos de resistência à colistina em isolados clínicos de *Acinetobacter baumannii* resistentes aos carbapenemos. MSc. Thesis. Universidade Nova de Lisboa. Instituto de Higiene e Medicina Tropical. https://run.unl.pt/handle/10362/116358. Accessed 20 May 2022.

Rolain, J.-M. *et al.* (2011). *Acinetobacter baumannii* resistant to colistin with impaired virulence: a case report from France. *J. Infect. Dis.* 204(7): 1146–1147. doi: org/10.1093/infdis/jir475.

Schmittgen, T.D. and Livak, K.J. (2008). Analyzing real-time PCR data by the comparative C_T method. *Nat. Protoc.* 3(6): 1101–1108. doi: 10.1038/nprot.2008.73.

Sherman, E.X., Wozniak, J.E. and Weiss, D.S. (2019). Methods to Evaluate colistin heteroresistance in *Acinetobacter baumannii*. *In* I. Biswas and P.N. Rather (eds) *Acinetobacter baumannii: Methods and Protocols*. New York, NY: Springer New York, pp. 39–50. doi: 10.1007/978-1-4939-9118-1_4.

Sievers, F. *et al.* (2011). Fast, scalable generation of high-quality protein multiple sequence alignments using Clustal Omega. *Mol. Syst. Biol.* 7: 539. doi: org/10.1038/msb.2011.75.

Society, M. (2022). Observing bacteria in a Petri dish. https://microbiologysociety.org/why-microbiology-matters/what-is-microbiology/bacteria/observing-bacteria-in-a-petri-dish.html. Accessed 24 September 2022.

Søgaard, P. (1985). Population analysis of susceptibility to cefotaxime in *Enterobacteriaceae*. *Acta Pathol. Microbiol. Scand. B.* 93(1-6): 365–369. doi: 10.1111/j.1699-0463.1985.tb02902.x.

van Soolingen, D., de Haas, P.E.W. and Kremer, K. (2001). Restriction fragment length polymorphism typing of mycobacteria. *Methods Mol. Med*. 54: 165-203. doi: 10.1385/1-59259-147-7:165.

Spellberg, B. and Rex, J.H. (2013). The value of single-pathogen antibacterial agents. *Nat. Rev. Drug Discov.* 12: 963. doi: 10.1038/nrd3957-c1.

Su, X.-Z. *et al.* (2005). AbeM, an H+-coupled *Acinetobacter baumannii* multidrug efflux pump belonging to the MATE family of transporters. *Antimicrob. Agents Chemother.* 49(10): 4362–4364. doi: 10.1128/AAC.49.10.4362-4364.2005.

Sun, L. *et al.* (2018). Droplet digital PCR-based detection of clarithromycin resistance in *Helicobacter pylori* isolates reveals frequent heteroresistance. *J. Clin. Microbiol.* 56(9): e00019-18. doi: 10.1128/JCM.00019-18.

Sutherland, R. and Rolinson, G.N. (1964). Characteristics of methicillin-resistant *staphylococci*', *J. Bacteriol*. 87(4): 887–899. 10.1128/jb.87.4.887-899.1964.

Valencia, R. *et al.* (2009). Nosocomial outbreak of infection with pan–drug-resistant *Acinetobacter baumannii* in a tertiary care university hospital. *Infect. Control Hosp. Epidemiol.* 30(3): 257–263. doi: 10.1086/595977.

Versalovic, J., Koeuth, T. and Lupski, J.R. (1991). Distribution of repetitive DNA sequences in eubacteria and application to fingerprinting of bacterial genomes. *Nucleic Acids Res*. 19(24): 6823–6831. doi: 10.1093/nar/19.24.6823.

Viehman, J.A., Nguyen, M.H. and Doi, Y. (2014). Treatment options for carbapenem-resistant and extensively drug-resistant *Acinetobacter baumannii* infections. *Drugs*. 74(12): 1315–1333. doi: 10.1007/s40265-014-0267-8.

Vila, J. and Pachón, J. (2008). Therapeutic options for *Acinetobacter baumannii* infections. *Expert Opin. Pharmacother*. 9(4): 587–599. doi: 10.1517/14656566.9.4.587.

Vila, J., Martí, S. and Sánchez-Céspedes, J. (2007). Porins, efflux pumps and multidrug resistance in *Acinetobacter baumannii*. *J. Antimicrob. Chemother.* 59(6): 1210–1215. doi: 10.1093/jac/dkl509.

Viveiros, M. *et al.* (2008). Demonstration of intrinsic efflux activity of *Escherichia coli* K-12 AG100 by an automated ethidium bromide method. *Int. J. Antimicrob. Agents*. 31(5): 458–462. doi: 10.1016/j.ijantimicag.2007.12.015.

Viveiros, M. *et al.* (2010). Evaluation of efflux activity of bacteria by a semi-automated fluorometric system. *In* S.H. Gillespie and T.D. McHugh (eds) *Antibiotic Resistance Protocols: Second Edition*. Totowa, NJ: Humana Press, pp. 159–172. doi: 10.1007/978-1-60327-279-7_12.

Vrancianu, C.O. *et al.* (2020). Escaping from ESKAPE. Clinical significance and antibiotic resistance mechanisms in *Acinetobacter baumannii*: a review. *Biointerface Res. Appl. Chem.* 11(1): 8190–8203. doi: 10.33263/BRIAC111.81908203.

Wiegand, I., Hilpert, K. and Hancock, R.E. (2008). Agar and broth dilution methods to determine the minimal inhibitory concentration (MIC) of antimicrobial substances. *Nat. Protoc.* 3: 163–175. doi: 10.1038/nprot.2007.521.

Wilson, L.A. (2006). Enterobacterial repetitive intergenic consensus (ERIC) sequences in *Escherichia coli*: evolution and implications for ERIC-PCR. *Mol. Biol. Evol.* 23(6): 1156–1168. doi: 10.1093/molbev/msj125.

Wong, D. *et al.* (2017). Clinical and pathophysiological overview of *Acinetobacter* infections: a century of challenges. *Clin. Microbiol. Rev.* 30(1): 409–447. doi: 10.1128/CMR.00058-16.

World Health Organization (2017). Antibacterial agents in clinical development: an analysis of the antibacterial clinical development pipeline, including tuberculosis. WHO/EMP/IAU/2017.11. World Health Organization. https://apps.who.int/iris/handle/10665/258965. Accessed 12 September 2022.

Yoon, E.-J. *et al.* (2015). Contribution of resistance-nodulation-cell division efflux systems to antibiotic resistance and biofilm formation in *Acinetobacter baumannii*. *mBio*. 6(2): e00309-15. doi: 10.1128/mBio.00309-15.

Zaidan, N., Hornak, J.P. and Reynoso, D. (2021). Extensively drug-resistant *Acinetobacter baumannii* nosocomial pneumonia successfully treated with a novel antibiotic combination', *Antimicrob. Agents Chemother.* 65(11): e00924-21. doi: 10.1128/AAC.00924-21.

Zheng, C. *et al.* (2015). Mixed infections and rifampin heteroresistance among *Mycobacterium tuberculosis* clinical isolates. *J. Clin. Microbiol.* 53(7): 2138–2147. doi: 10.1128/JCM.03507-14.

6. Appendix

Appendix 1. Antibiotic susceptibility profile of the *A. baumannii* clinical strains and strain-variants under study, determined by the Kirby-Bauer method.

Estirpe	AMP[(1)]	AMC[(1)]	OX[(2)]	PRL	TZP	CAZ	FEP	CTX	CRO	DOR	IMP	MEM	CN	TOB	AK	NET[(3)]	DO	MH	TE	TGC[(4)]	LEV	CIP	SXT
ATCC19606	R	R	R	I	S	S	S	I	I	S	S	S	S	S	S	R	S	S	S	S	S	S	R
Ab10-6	R	R	R	R	R	I	S	R	R	R	R	R	R	R	R	R	I	S	R	S	R	R	R
L Variant	R	R	R	R	R	R	I	R	R	R	R	R	R	R	R	R	R	R	R	S	R	R	R
S Variant	R	R	R	R	R	R	I	R	R	R	R	R	R	R	R	R	R	R	R	S	R	R	R
XS Variant	R	R	R	R	R	R	I	R	R	R	R	R	R	R	R	R	R	R	R	S	R	R	R

R, resistant; I, Susceptible, increased exposure; S, susceptible. Antibiotic abbreviations are shown as inscription on the respective discs. AMP, ampicillin; AMC, amoxicillin/clavulanic acid; PRL, piperacillin; TZP, piperacillin-tazobactam; OX, oxacillin; CAZ, ceftazidime; CTX, cefotaxime; CRO, ceftriaxone, FEP, cefepime; IPM, imipenem; MEM, meropenem; DOR, doripenem; AK, amikacin; CN, gentamicin; NET, netilmicin; TOB, tobramycin, DO, doxycycline, MH minocycline; TE, tetracycline; TGC, tigecycline; LEV, levofloxacin; CIP, ciprofloxacin; SXT, trimethoprim-sulfamethoxazole. (1) Breakpoints for *Acinetobacter* spp. not defined, interpretation based on breakpoints for *Enterobacteriaceae* according to CLSI guidelines (CLSI, 2018). (2) There are no breakpoints for oxacillin for *Acinetobacter* spp. (3) “Breakpoints” according to EUCAST standards (EUCAST, 2017). (4) Zone diameters interpretation based on the US Food and Drug Administration breakpoints for susceptibility (Pharmaceutics, 2005).